Importance of boundary conditions for fluctuation-induced forces between colloids at interfaces

Hartwig Lehle[1,2] and Martin Oettel[1,2,3]
[1]*Max-Planck-Institut für Metallforschung, Heisenbergstrasse 3, D-70569 Stuttgart, Germany*
[2]*Institut für Theoretische und Angewandte Physik, Universität Stuttgart, Pfaffenwaldring 57, D-70569 Stuttgart, Germany*
[3]*Institut für Physik, WA 331, Johannes-Gutenberg-Universität Mainz, 55099 Mainz, Germany*
(Received 24 August 2006; revised manuscript received 10 November 2006; published 12 January 2007)

We calculate the effective fluctuation-induced force between spherical or disklike colloids trapped at a flat, fluid interface mediated by thermally excited capillary waves. This Casimir-type force is determined by the partition function of the system which in turn is calculated in a functional integral approach, where the restrictions on the capillary waves imposed by the colloids are incorporated by auxiliary fields. In the long-range regime the fluctuation-induced force is shown to depend sensitively on the boundary conditions imposed at the three-phase contact line between the colloids and the two fluid phases. Separating the colloid fluctuations from the fluctuations of the capillary wave field leads to competing repulsive and attractive contributions, respectively, which give rise to cancellations of the leading terms. In a second approach based on a multipole expansion of the Casimir interaction, these cancellations can be understood from the vanishing of certain multipole moments enforced by the boundary conditions. We also discuss the connection of the different types of boundary conditions to certain external fields acting on the colloids which appear to be realizable by experimental techniques such as the laser tweezer method.

DOI: 10.1103/PhysRevE.75.011602 PACS number(s): 68.03.Kn, 82.70.Dd

I. INTRODUCTION

The structure formation of nanoscopic colloidal particles adsorbed at fluid interfaces has attracted increasing interest in recent years because of the various applications such systems exhibit, as in the design of nanoscale devices [1] (e.g., for optical applications), and also because of the physical insights offered, e.g., for the understanding of protein aggregation on cell membranes. The practical importance arises from the fact that nano- and microcolloids are very effectively trapped by fluid interfaces [2]. The high stability of partially wetting colloids (with their size ranging from nanometers to micrometers) at interfaces enables the formation of two-dimensional ordered structures and also of rather complex mesoscale patterns (cf. Refs. [3–11]). In spite of the numerous experimental and theoretical efforts in the last decade, the nature of the effective forces between the colloids governing the arrangement of the colloids trapped at the interface is not fully understood yet. This holds in particular for the mesoscale pattern formation which points to sizable and quite long-ranged attractions between the colloids. For the colloidal interactions at interfaces three different regimes may be distinguished. For colloid sizes of about $0.5-5\ \mu$m, capillary forces are important. Though gravity is known to be unimportant in this regime, electrostatic forces (either caused only by the charge distributions on the colloid surface and the fluid phases, or additionally imposed by an external field) may lead to interfacial deformations and, hence, to considerable capillary interactions [12–14]. In this regime, also strong effects of colloid surface inhomogeneities leading to an undulated three-phase contact line appear to be relevant [7]. In the opposite limit of colloid sizes of a few nanometers, effects of interparticle correlations within the interface become important and determine the structural properties of the system. In this regime the colloidal interactions should be treated by truly microscopic fluid theories like density functional or inhomogeneous integral equation approaches (for a general scheme, see Ref. [15], and for results on correlations within a free interface, see Refs. [16,17]). In between these two regimes, the microscopic one which must be tackled with the full power of classical statistical mechanics and the macroscopic one where thermal fluctuations appear to be unimportant, a coarse-grained picture of the fluctuating fluid interface should be applied. Within such a picture, the properties of fluid interfaces are very well described by an effective capillary wave Hamiltonian which governs both the equilibrium interface configuration and the thermal fluctuations (capillary waves) around this equilibrium (or mean-field) position. The fluctuation spectrum of the capillary waves will be modified by colloids trapped at the interface and therefore leads to fluctuation-induced forces between them. Since capillary waves are the Goldstone modes of the broken translational symmetry pertaining to a free interface, their correlations are long ranged (in the absence of gravity) and the corresponding fluctuation-induced forces are a manifestation of the well-known Casimir effect in two dimensions [19]. In the case of anisotropic colloids (rods) these forces have been evaluated in Ref. [20] and shown to lead to an orientational dependence. Furthermore we note that there is numerous work on the force between inclusions on membranes where the membrane shape fluctuations take the role of capillary waves; see, e.g., Refs. [20,21]. In this paper, we shall address the fluctuation-induced effects of capillary waves on rotationally symmetric colloids, i.e., spherical or disklike ones, and pay special attention to the effects of the boundary conditions at the three-phase contact line (where the fluid interface meets the colloid surface) on the large-distance behavior of the fluctuation-induced force. In previous work [22] we have established the independence of the short-distance behavior of the boundary conditions. For colloids at contact, the fluctuation-induced force is attractive and diverging, albeit the divergence is somewhat slower than for the ubiquitous van der Waals (vdW) forces. However, as

discussed in Ref. [22], the fluctation-induced force dominates for specially prepared systems (such as index-matched ones) and hence it leads to colloidal aggregation at the interface.

Regarding the influence of the boundary conditions on the long-ranged behavior of the Casimir force, we note a previous study on the force between spheres in a fluctuating medium described by a free scalar field in arbitrary dimension D [23]. Using a terminology borrowed from electrostatics, the scalar "field" corresponds to the potential and if the spheres are presumed to be metallic, one can distinguish two types of boundary condition: (i) the spheres are grounded, corresponding to zero potential at their surface (Dirichlet boundary conditions) and (ii) the spheres are isolated with constant charge, in which case one averages over the surface potential. The asymptotic Casimir force between two spheres at distance d strongly depends on the type of boundary condition; in case (i) the author finds $F_{\text{ground}} \sim 1/d^{2(D-2)+1}$ and for case (ii) $F_{\text{iso}} \sim 1/d^{2D+1}$. In relation to this study, our present work is only concerned with the case $D=2$. The boundary conditions introduced above correspond to the physically realizable conditions of a fixed colloid with pinned three-phase contact line (grounded case) and a vertically fluctuating colloid with pinned contact line (isolated case). Furthermore we will identify two more physically realizable boundary conditions (arbitrarily fluctuating colloid with pinned contact line and colloid with freely fluctuating contact line) which lead to different results for the Casimir force again. Also we will find that in $D=2$ the general result for F_{ground} is modified since care is needed to perform the limit to a massless fluctuating field. We will elucidate the appearance of the leading terms in an asymptotic expansion of the Casimir force from two different computational schemes. In the first one, we split the partition function into two separate factors corresponding to the effect of (i) the fluctuations of the colloid degree of freedoms and (ii) the fluctuations of the interface position. The statistical weight of the configurations (i) is determined by the mean-field energy of the interface corresponding to boundary conditions prescribed by the fluctuating colloid; therefore we call (i) the mean-field part for brevity. On the other hand, the statistical weight of the configurations (ii) is determined purely by the energy of the fluctuating interface with Dirichlet boundary conditions and is independent of the colloid degrees of freedom. We call (ii) the fluctuation part in short. The mean-field part leads to a repulsive and the fluctuation part to an attractive contribution to the Casimir interaction and the leading nonvanishing term in the asymptotic behavior for large colloid separations then strongly depends on the type of boundary conditions under consideration. This splitting of the partition function also allows for a very efficient numerical calculation of the fluctuation-induced force in the whole range of colloid separations and for its analytical determination in the short-range limit. In a second, alternative approach (with no such separation of the fluctuating variables) the strong dependence of the long-range asymptotics on the boundary conditions can be understood from an expansion of the interaction between the colloids into fluctuating auxiliary multipoles, as in Ref. [23]. One can relate each type of boundary conditions to a suppression of certain auxiliary multipoles on the colloids and the leading term of the Casimir force is obtained from the first nonvanishing multipole-multipole interaction.

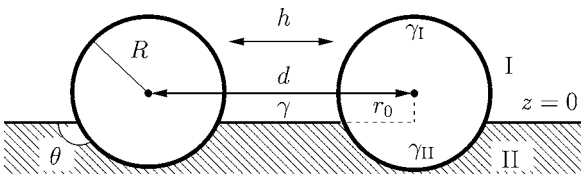

FIG. 1. Side view of the reference configuration (here the colloids are assumed to be spheres).

The paper is organized as follows. In Sec. II we will introduce the model system by an effective Hamiltonian. We will show how the partition function can be calculated via functional integrals in two distinct ways mentioned above and how the various boundary conditions can be implemented. Then we will compute the corresponding functional integrals in Secs. III–V in the asymptotic regimes of long and short colloid separations d and numerically in the full range of d, respectively, and compare analytical with numerical results in the discussion part, Sec. VI. Finally we will also discuss possible experimental tests for this type of Casimir force through the implications of an additional external potential for the colloids, which may, e.g., be realized by optical tweezers.

II. MODEL

In this section we derive an effective Hamiltonian for the free energy changes associated with thermally excited height fluctuations of the interface between two fluid phases I and II at which two nano- or microscopic colloids are trapped. As described above, this configuration is very stable against thermal fluctuations for colloids with a partially wetting surface. The colloids are assumed to be either spherical with radius R or disklike with radius R and thickness H. In the absence of charges and for colloid sizes $R \lesssim 1$ μm the weight of the particles can be neglected. Thus the equilibrium configuration of minimal free energy is the flat interface and spherical colloids are positioned such that Young's law holds at the horizontal three-phase contact line which is a circle with radius $r_0 = R \sin\theta$. Young's angle, measured through phase II (assumed to be of higher density than phase I), is determined by $\cos\theta = (\gamma_{\text{I}} - \gamma_{\text{II}})/\gamma$ where γ is the surface tension of the interface between I and II, and $\gamma_{\text{I[II]}}$ is the surface tension between the colloid and phase I (II), respectively (see Fig. 1). For disklike colloids, the contact line is either the upper ($\theta < \pi/2$) or lower ($\theta > \pi/2$) circular edge, so that its radius is given by $r_0 = R$. For both spheres and disks the cross section of the colloids with the flat interface is given by the interior of a circle which we refer to as $S_{i,\text{ref}}$ below, and, therefore both cases can be treated within the same model in the following. We take the flat interface $S_{\text{men,ref}}$ as the reference configuration with respect to which free energy changes are measured, and choose it to be the plane $z=0$ with the two circular holes $S_{i,\text{ref}}$ of radius r_0 in it: $S_{\text{men,ref}} = \mathbb{R}^2 \setminus \cup_i S_{i,\text{ref}}$ (see Fig. 2). Deviations from the planar reference interface $z=0$

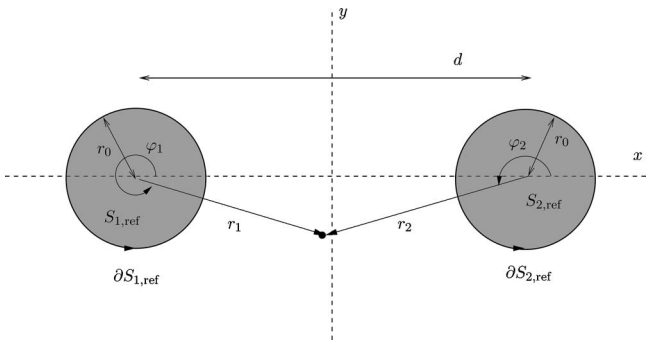

FIG. 2. Reference configuration with two circles $S_{i,\mathrm{ref}}$ representing the reference contact line on the colloid surfaces (here the colloids may be disks or spheres).

are assumed to be small and without overhangs or bubbles. That allows using the Monge representation $[x,y,z=u(x,y)]=[\mathbf{x},z=u(\mathbf{x})]$ as a parametrization of the actual interface positions. The free energy costs for thermal fluctuations around the flat reference interface are determined by the the change in interfacial energy of all interfaces (I/II, colloid/I, and colloid/II):

$$\mathcal{H}_{\mathrm{tot}} = \gamma \Delta A_{\mathrm{men}} + \gamma_{\mathrm{I}} \Delta A_{\mathrm{I}} + \gamma_{\mathrm{II}} \Delta A_{\mathrm{II}}. \tag{1}$$

The first term in Eq. (1) expresses the energy needed for creating the additional meniscus area associated with the height fluctuations and is given by

$$\gamma \Delta A_{\mathrm{men}} = \gamma \int_{S_{\mathrm{men}}} d^2x \sqrt{1+(\nabla u)^2} - \gamma \int_{S_{\mathrm{men,ref}}} d^2x$$
$$\approx \frac{\gamma}{2} \int_{S_{\mathrm{men,ref}}} d^2x (\nabla u)^2 + \gamma \Delta A_{\mathrm{proj}}. \tag{2}$$

In Eq. (2), S_{men} is the meniscus area projected onto the plane $z=0$ (where the reference interface is located) and $S_{\mathrm{men,ref}}$ is the meniscus in the reference configuration mentioned above. $\Delta A_{\mathrm{proj}}=\int_{S_{\mathrm{men}}\setminus S_{\mathrm{men,ref}}} d^2x$ is the change in projected meniscus area with respect to the reference configuration. In the second line we have applied a small gradient expansion that is valid for slopes $|\nabla u| \ll 1$ and which provides the long-wavelength description of the interface fluctuations we are interested in. Note that the first line of Eq. (2) constitutes the drumhead model which is well known in the renormalization group analysis of interface problems, but is also used for the description of elastic surfaces (cf. Ref. [18]).

As discussed in the Introduction, the center of colloid i may fluctuate vertically (measured by h_i) around the reference position as well as the contact line itself may do. This leads to changes in the interfacial areas colloid/I (II) [$\Delta A_{\mathrm{I(II)}} \neq 0$ in Eq. (1)]. In order to determine the corresponding energy costs we introduce the vertical position of the contact line at colloid i as a function of the polar angle φ_i, defined on the reference contact line circles $\partial S_{i,\mathrm{ref}}$, by its Fourier expansion

$$f_i = u(\partial S_{i,\mathrm{ref}}) = \sum_{m=-\infty}^{\infty} P_{im} e^{im\varphi_i} \tag{3}$$

and refer to the Fourier coefficients P_{im} as boundary multipole moments below. Since f_i is real, we have $P_{im}=P_{i-m}^{*}$. Following Ref. [13], the free energy changes associated with ΔA_{proj} and $\Delta A_{\mathrm{I(II)}}$ can be expanded up to second order in h_i and f_i, and may therefore be collected in a boundary Hamiltonian $\mathcal{H}_{i,\mathrm{b}}$ (see Appendix A):

$$\mathcal{H}_{\mathrm{b},i}[f_i,h_i] = \gamma \Delta A_{\mathrm{proj}} + \gamma_{\mathrm{I}} \Delta A_{\mathrm{I}} + \gamma_{\mathrm{II}} \Delta A_{\mathrm{II}}$$
$$= \frac{\pi\gamma}{2} \left(2(P_{i0}-h_i)^2 + 4 \sum_{m\geq 1} |P_{im}|^2 \right). \tag{4}$$

Putting Eqs. (1), (2), and (4) together, the total free energy change is the sum

$$\mathcal{H}_{\mathrm{tot}} = \mathcal{H}_{\mathrm{cw}} + \mathcal{H}_{\mathrm{b},1} + \mathcal{H}_{\mathrm{b},2} = \frac{\gamma}{2} \int_{S_{\mathrm{men,ref}}} d^2x (\nabla u)^2 + \mathcal{H}_{\mathrm{b},1} + \mathcal{H}_{\mathrm{b},2} \tag{5}$$

of the capillary wave Hamiltonian $\mathcal{H}_{\mathrm{cw}}$ which describes the free energy differences associated with the additional interfacial area created by the height fluctuations, and the boundary Hamiltonians $\mathcal{H}_{\mathrm{b},i}$ combining all effects related to fluctutations of the three-phase contact line on the colloid surfaces. As is well known, the Hamiltonian $\mathcal{H}_{\mathrm{cw}}$ is plagued with both a short-wavelength and a long-wavelength divergence which, however, can be treated by physical cutoffs. The natural short-wavelength cutoff is set by the molecular length scale σ of the fluid at which the capillary wave model ceases to remain valid. The long-wavelength divergence is reminiscent of the fact that the capillary waves are Goldstone modes. Of course, in real systems the gravitational field provides a natural damping for capillary waves. Accounting also for the costs in gravitational energy associated with the interface height fluctuations, therefore, introduces a long-wavelength cutoff and leads to an additional term ("mass term") in the capillary wave Hamiltonian,

$$\mathcal{H}_{\mathrm{cw}} = \frac{\gamma}{2} \int_{S_{\mathrm{men,ref}}} d^2x \left((\nabla u)^2 + \frac{u^2}{\lambda_c^2} \right). \tag{6}$$

Here the capillary length is given by $\lambda_c=[\gamma/(|\rho_{\mathrm{II}}-\rho_{\mathrm{I}}|g)]^{1/2}$, where ρ_i is the mass density in phase i and g is the gravitational constant. Usually, in simple liquids, λ_c is in the range of millimeters and, therefore, is by far the longest length scale in the system. In fact, here it plays the role of a long-wavelength cutoff of the capillary wave Hamiltonian $\mathcal{H}_{\mathrm{cw}}$, and we will discuss our results in the limit $\lambda_c \gg R$ and $\lambda_c \gg d$. However, as we will see below, care is required when taking the limit $\lambda_c \to \infty$ (corresponding to $g \to 0$), since logarithmic divergencies appear [24]. Another common way to introduce a long-wavelength cutoff is the finite size L of any real system. As discussed in Ref. [13], the precise way of incorporating the long-wavelength cutoff is unimportant for the effects on the colloidal length scale. As an example, in both approaches the width of the interface related to the cap-

illary wave is logarithmically divergent, $\langle u(0)^2\rangle \sim \ln \lambda_c[L]/\sigma$.

Via the integration domain of $\mathcal{H}_{\mathrm{cw}}$, the total Hamiltonian of the system, Eq. (5), implicitly depends on the geometric configuration. This leads to a free energy which depends on the mean distance d between the colloid centers and gives rise to an effective force $F(d)=-(\partial\mathcal{F})/(\partial d)$ as a function of the mean local distance between the colloid centers which is determined by the free energy $\mathcal{F}(d)=-k_BT\ln\mathcal{Z}(d)$. The partition function $\mathcal{Z}(d)$ is obtained by a functional integral over all possible interface configurations u and f_i; the boundary configurations are included by δ-function constraints,

$$\mathcal{Z}=\mathcal{Z}_0^{-1}\int \mathcal{D}u\,\exp\left(-\frac{\mathcal{H}_{\mathrm{cw}}[u]}{k_BT}\right)\prod_{i=1}^{2}\int \mathcal{D}f_i \prod_{\mathbf{x}_i\in\partial S_{i,\mathrm{ref}}} \times\delta[u(\mathbf{x}_i)-f_i(\mathbf{x}_i)]\exp\left(-\frac{\mathcal{H}_{\mathrm{b},i}[f_i,h_i]}{k_BT}\right). \tag{7}$$

Here $\mathcal{Z}_0$ is a normalization factor such that $\mathcal{Z}(d\to\infty)=1$ and ensures a proper regularization of the functional integral. Via the δ functions the interface field u is coupled to the contact line height f_i and therefore, the boundary Hamiltonians $\mathcal{H}_{i,\mathrm{b}}$ have a crucial influence on the resulting effective interaction between the colloids as we will see below. In the next section we discuss possible situations for the boundary conditions at the three-phase contact line and specify the corresponding integration measure $\mathcal{D}f_i$.

A. Boundary conditions at the three-phase contact line

We shall discuss two different realizations of the boundary conditions for the contact line, as follows.

Case (A). The contact lines and the vertical colloid positions fluctuate freely; this corresponds to the physical situation of smooth, spherical colloids. In this case, the integration measure is given by $\mathcal{D}f_i=\int dh_i\Pi_m dP_{im}$ and encompasses integration over all boundary multipole moments.

Case (B). The contact lines (the circles $\partial S_{i,\mathrm{ref}}$ in the reference configuration) are pinned to the colloid surface. This corresponds to disklike colloids or Janus spheres consisting of two different materials, or to colloids with a very rough surface. Within the pinning case, we furthermore distinguish the following three situations.

(B1) The colloid positions are frozen; thus there are no integrations over the boundary terms.

(B2) The vertical positions of the colloids fluctuate freely; thus boundary monopoles must be included in the integration measure so that $\mathcal{D}f_i=dh_idP_{i0}\delta(P_{i0}-h_i)$.

(B3) The vertical position and the orientation of the colloids (tilts) fluctuate freely. Up to second order in the tilts this corresponds to the inclusion of boundary dipoles in the integration measure; thus $\mathcal{D}f_i=dh_idP_{i0}dP_{i1}dP_{i-1}\delta(P_{i0}-h_i)$.[1]

The δ function expresses the pinning condition.

These boundary conditions are sketched in Fig. 3. Note that Df_i is not necessarily identical for the two colloids $i=1,2$ in the expression (7) for the partition function. This allows for various combinations of boundary conditions which leads to a different behavior for the effective force, respectively, as we will show in Sec. III.

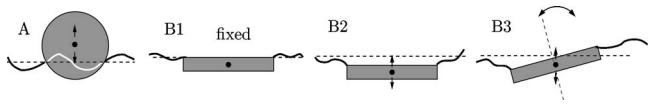

FIG. 3. Sketch of the various boundary conditions. For (B1)–(B3), the disks may be replaced by Janus spheres.

In the following subsections we introduce the two distinct schemes to compute the partition function $\mathcal{Z}(d)$ in Eq. (7) which allows us to discuss the results from different perspectives. The first one is based on the splitting of $\mathcal{Z}$ into the mean-field part (fluctuating colloid degrees of freedom determining boundary conditions for a mean-field interface) and the fluctuation part (only interface fluctuations), whereas for the second one we extend the fluid interface—artificially—to the interior of the reference circles $S_{i,\mathrm{ref}}$.

B. Mean-field and fluctuation parts

As the capillary wave Hamiltonian is Gaussian in the field u of the local interface position, a standard procedure for the evaluation of the functional integral (7) is the decomposition into a mean-field and a fluctuation part,

$$u=u_{\mathrm{mf}}+v. \tag{8}$$

The mean-field part solves the Euler-Lagrange equation of the capillary wave Hamiltonian $\mathcal{H}_{\mathrm{cw}}$,

$$(-\Delta+\lambda_c^{-2})u_{\mathrm{mf}}=0, \tag{9}$$

with the boundary condition $u_{\mathrm{mf}}|_{\partial S_{i,\mathrm{ref}}}=f_i$. Consequently the fluctuation part is pinned to zero at the contact line, $v|_{\partial S_{i,\mathrm{ref}}}=0$. Then the partition sum $\mathcal{Z}=\mathcal{Z}_{\mathrm{fluc}}\mathcal{Z}_{\mathrm{mf}}$ separates into a product of a fluctuation part independent of the boundary conditions, and a mean-field part depending on the boundary conditions [which may fluctuate themselves; see the cases (A), (B2), and (B3)]:

$$\mathcal{Z}_{\mathrm{fluc}}=\mathcal{Z}_0^{-1}\int \mathcal{D}v\prod_{i=1}^{2}\prod_{\mathbf{x}_i\in\partial S_{i,\mathrm{ref}}}\delta(v(\mathbf{x}_i))\exp\left(-\frac{\mathcal{H}_{\mathrm{cw}}[v]}{k_BT}\right),$$

$$\mathcal{Z}_{\mathrm{mf}}=\prod_{i=1}^{2}\int \mathcal{D}f_i\exp\left(-\frac{\gamma}{2k_BT}\sum_i\int_{\partial S_{i,\mathrm{ref}}} d\ell_i f_i(\mathbf{x}_i)\times[\partial_n u_{\mathrm{mf}}(\mathbf{x}_i)]\right)\exp\left(-\frac{\mathcal{H}_{\mathrm{b},i}[f_i,h_i]}{k_BT}\right). \tag{10}$$

The first exponential in $\mathcal{Z}_{\mathrm{mf}}$ stems from applying Gauss's theorem to the energy associated with u_{mf}. In this term $\partial_n u_{\mathrm{mf}}$ denotes the normal derivative of the mean-field solution toward the interior of the circle $\partial S_{i,\mathrm{ref}}$.

For intermediate asymptotic distances between the colloids ($r_0\ll d\ll\lambda_c$), $\mathcal{Z}_{\mathrm{fluc}}$ and $\mathcal{Z}_{\mathrm{mf}}$ are analyzed separately in Secs. III A and III B, respectively.

[1]Since $P_{im}=P_{i-m}^*$, the real and imaginary parts of $P_{i\pm m}$ are not independent of each other, and therefore we define the measure $dP_{im}dP_{i-m}\equiv d\,\mathrm{Re}\,P_{im}d\,\mathrm{Im}\,P_{i-m}$.

This procedure is equivalent to the standard calculation of the quantum mechanical path integral for a single particle in a harmonic potential. The mean-field part corresponds to the classical action and the fluctuation part evaluated becomes the fluctuation determinant (see, e.g., Ref. [25]).

C. Alternative approach (Kardar's method)

An alternative scheme to calculate the partition function of the two colloids and the fluctuating interface without splitting it into a mean-field and fluctuation part can be devised if the interface height field $u(x,y)$ which enters the functional integral for $\mathcal{Z}$ is extended to the interior of the circles $S_{i,\mathrm{ref}}$. Thus the measure of the functional integral for $\mathcal{Z}$ is extended by $\mathcal{D}u(\mathbf{x})|_{\mathbf{x}\in S_{i,\mathrm{ref}}}$ and the integration domain in the capillary wave Hamiltonian is enlarged to encompass the whole $\mathbb{R}^2$. We note that physically the free energy of the system must not change since in the interior of $S_{i,\mathrm{ref}}$ the interface is pinned to the colloid surface. A method similar to this ansatz was introduced in Ref. [20] by Kardar *et al.* which investigates effective forces between rods on fluctuating membranes and films, and therefore we refer to it as Kardar's method in the following.

On the colloid surfaces, the interface height field is given by the three phase contact line, $u(\partial S_{i,\mathrm{ref}})\equiv f_i$. We extend u continuously to the interior of the circles $S_{i,\mathrm{ref}}$ via

$$u(S_{i,\mathrm{ref}}) \equiv f_{i,\mathrm{ext}}(r_i,\varphi_i) = \sum_m \left(\frac{r_i}{r_0}\right)^{|m|} P_{im} e^{im\varphi_i}, \tag{11}$$

where r_i and φ_i are the polar coordinates with respect to circle $S_{i,\mathrm{ref}}$ and where the boundary multipoles satisfies $P_{im}=P^*_{i-m}$. Note that the choice of $u(S_{i,\mathrm{ref}})$ is not unique since the continuity at the boundaries $\partial S_{i,\mathrm{ref}}$ is the only requirement. The specific choice in Eq. (11) is convenient for the further calculations since $\Delta f_{i,\mathrm{ext}}=0$ in $S_{i,\mathrm{ref}}\backslash\partial S_{i,\mathrm{ref}}$. Extending the integration domain of the capillary wave Hamiltonian in Eq. (5), $\Omega=\mathbb{R}^2\backslash\cup_i S_{i,\mathrm{ref}}\to\mathbb{R}^2$ generates an additional energy contribution

$$-H_{i,\mathrm{corr}} = \frac{\gamma}{2}\int_{S_{i,\mathrm{ref}}} d^2x\left((\nabla u)^2+\frac{u^2}{\lambda_c^2}\right) \simeq 2\pi\gamma\sum_{m\geqslant 1} m|P_{im}|^2. \tag{12}$$

In Eq. (12) we have already omitted the contributions from the gravitational term in $\mathcal{H}_{\mathrm{cw}}$ which are of order $(r_0/\lambda_c)^2\ll 1$. From Eq. (12) we see that the additional terms created by the extension of the integration domain of the capillary wave Hamiltonian $\mathcal{H}_{\mathrm{cw}}$ are not constant in the—possibly fluctuating—boundary multipole moments P_{im} and therefore lead to artificial contributions to the partition function $\mathcal{Z}$. These unphysical contributions have to be corrected by adding $H_{i,\mathrm{corr}}$ to the extended capillary wave Hamiltonian $H_{\mathrm{cw}}[\Omega\equiv\mathbb{R}^2]$. The total Hamiltonian then reads

$$H_{\mathrm{tot}} = H_{\mathrm{cw}} + \sum_{i=1}^{2}[H_{i,\mathrm{b}}+H_{i,\mathrm{corr}}]. \tag{13}$$

As in the previous sections the partition function is written as a functional integral over all possible configurations of the interface position u and the boundary lines, expressed by f_i,

$$\mathcal{Z} = \mathcal{Z}_0^{-1}\int \mathcal{D}u\prod_{\mathrm{i}=1}^{2}\int \mathcal{D}f_i \prod_{\mathbf{x}_i\in S_{i,\mathrm{ref}}}\delta[u(\mathbf{x}_i)-f_{i,\mathrm{ext}}(\mathbf{x}_i)] \times\exp\left(-\frac{\mathcal{H}_{\mathrm{tot}}[f_i,u]}{k_{\mathrm{B}}T}\right), \tag{14}$$

where the product over the δ functions enforces the pinning of the interface at the positions of the colloids. In contrast to Eq. (7), these product extends over all $\mathbf{x}\in S_{i,\mathrm{ref}}$ instead of $\partial S_{i,\mathrm{ref}}$, only. The analysis of $\mathcal{Z}$ in this form for intermediate asymptotic distances d is presented below in Sec. III C.

III. LONG-RANGE BEHAVIOR

In this section we calculate analytical expressions for the fluctuation-induced force in the intermediate asymptotic regime $r_0\ll d\ll\lambda_c$. For the first approach, this necessitates the evaluation of the partition functions for the fluctuation and the mean-field part separately (Secs. III A and III B, respectively). For the Kardar method, the partition function and therefore the fluctuation force can be calculated directly (Sec. III C). For convenience, we have summarized the final results for the effective Casimir force at the beginning of this section. Readers only interested in these may skip the computational details in Secs. III A–III C and directly proceed to the discussion of the short-range behavior of the Casimir force in Sec. IV.

Summary of this section's results. Because $\mathcal{Z}=\mathcal{Z}_{\mathrm{fluc}}\mathcal{Z}_{\mathrm{mf}}$, the total effective force F is obtained as $F=F_{\mathrm{fluc}}+F_{\mathrm{mf}}$ and depends on the type of boundary conditions through F_{mf} only. In all cases the large-d expansion of the mean-field part of the partition sum (with $\lambda_c\to\infty$) leads to a repulsive F_{mf}, whereas the fluctuation contribution F_{fluc} is attractive. Thus the total Casimir force between the colloids is determined by an interesting interplay between the two-dimensional "bulk" fluctuations and one-dimensional boundary fluctuations influencing the two-dimensional bulk by a change of the mean field. Combining the expansions of the mean-field and the fluctuation free energies [cf. Eqs. (36) and (22) in Secs. III A and III B respectively], the asymptotic form of the total Casimir force can be written as a power series in r_0/d,

$$F(d) = -\frac{k_{\mathrm{B}}T}{2}\frac{\partial}{\partial d}\sum_n [f_{2n}^{\mathrm{mf}}+f_{2n}^{\mathrm{fluc}}]\left(\frac{r_0}{d}\right)^{2n}. \tag{15}$$

In Table I we provide the resulting Casimir forces for various combinations of the boundary conditions from Sec. II A For a pinned contact line and fixed colloids, $F_{\mathrm{mf}}=0\to f_{2n}^{\mathrm{mf}}=0$, and the full Casimir force is given by F_{fluc} [Eq. (23) in Sec. III A below]. For fluctuating boundary conditions, however, the leading attractive coefficients are canceled by repulsive ones from the mean-field part, $f_{2n}^{\mathrm{fluc}}=-f_{2n}^{\mathrm{mf}}$, up to a certain order n which depends on the boundary conditions considered. Nevertheless, the total Casimir force is always attractive for like boundary conditions. For mixed boundary conditions, the total Casimir force is repulsive only if the cases of pinned contact line (B1)–(B3) for one colloid are combined with the case (A) of an unpinned contact line for the other colloid.

TABLE I. Total Casimir force (in units of k_BT/r_0) for various combinations of boundary conditions for $\lambda_c \to \infty$

	Colloid 2			
Colloid 1	(B1)	(B2)	(B3)	(A)
(B1)	$-\frac{1}{2}\frac{1}{(d/r_0)\ln(d/r_0)}$	$-4\left(\frac{r_0}{d}\right)^5$	$-12\left(\frac{r_0}{d}\right)^7$	$+4\left(\frac{r_0}{d}\right)^7$
(B2)		$-4\left(\frac{r_0}{d}\right)^5$	$-12\left(\frac{r_0}{d}\right)^7$	$+4\left(\frac{r_0}{d}\right)^7$
(B3)			$-72\left(\frac{r_0}{d}\right)^9$	$+24\left(\frac{r_0}{d}\right)^9$
(A)				$-8\left(\frac{r_0}{d}\right)^9$

This resembles the rule known from the critical Casimir effect that like boundaries attract and unlike repel each other [26].

Alternatively, the expansion coefficients in Eq. (15) can be calculated directly within the Kardar approach, which yields $f_{2n}^{\text{Kardar}}=f_{2n}^{\text{mf}}+f_{2n}^{\text{fluc}}$. As demonstrated below, the coefficients f_{2n}^{Kardar} can be regarded as two-dimensional multipole interaction coefficients between auxiliary fields (or "charge" densities) defined on $S_{i,\text{ref}}$. Here $n=p_1+p_2$ and p_i is the order of the auxiliary multipole residing on colloid i. The interaction between the auxiliary multipoles Ψ_{1p_1} and Ψ_{2p_2} scales like $(r_0/d)^{p1+p2}$ [cf. Eq. (44) in Sec. III C below]. As shown in Sec. III C, the different boundary conditions lead to certain constraints on the auxiliary multipoles. In particular, we find that a fluctuating boundary monopole corresponds to a vanishing auxiliary monopole and a fluctuating boundary dipole corresponds to a vanishing auxiliary dipole. Higher-order boundary multipole fluctuations, however, do not lead to further multipole cancellations but lead to a change of amplitude in the leading term. [Compare, e.g., the results for the boundary type combinations (A)-(A) and (B3)-(B3) in Table 1.] Thus, the leading order of the total fluctuation-induced force between the two colloids is determined by the first nonvanishing auxiliary multipole moments Ψ_{ip_i} and gives rise to a force $F(d)\propto 1/d^{2(p_1+p_2)+1}$ (for $p_1,p_2>0$) or $F(d)\propto 1/(d\ln d)$ (for $p_1=p_2=0$). If only one of the p_i is zero, the logarithmic corrections stemming from the monopole interactions vanish in the limit $\lambda_c\to 0$. Then the Casimir force is determined by the next-to-leading multipole interaction, i.e., a dipole-dipole interaction in the case of (B1)-(B2) and a dipole-quadrupole interaction for (B1)-(B3) or (B1)-(A) boundary conditions.

A. Fluctuation part

The fluctuation part appears for all cases of like and mixed boundary conditions. In the case (B1)-(B1) (pinned contact line with frozen colloids) it constitutes the full result for the partition function because $u_{\text{mf}}=0$ and $\mathcal{Z}_{\text{mf}}=1$. We express the δ functions in the fluctuation part of the partition function (10) by their integral representation via auxiliary fields $\psi_i(\mathbf{x}_i)$ defined on the interface boundaries $\partial S_{i,\text{ref}}$. This enables us to integrate out the field u leading to

$$\mathcal{Z}_{\text{fluc}}=\int\prod_{i=1}^{2}\mathcal{D}\psi_i\exp\left(-\frac{k_BT}{2\gamma}\sum_{i,j=1}^{2}\times\int_{\partial S_{i,\text{ref}}}d\ell_i\int_{\partial S_{j,\text{ref}}}d\ell_j\psi_i(\mathbf{x}_i)G(|\mathbf{x}_i-\mathbf{x}_j|)\psi_j(\mathbf{x}_j)\right), \tag{16}$$

where $d\ell_i$ is the infinitesimal line segment on the circles $\partial S_{i,\text{ref}}$. In Eq. (16) we introduced the Greens function of the operator $(-\Delta+\lambda_c^{-2})$ which is given by $G(\mathbf{x})=K_0(|\mathbf{x}|/\lambda_c)/(2\pi)$ where K_0 is the modified Bessel function of the second kind. In the range $d/\lambda_c\ll 1$ and $r_0/\lambda_c\ll 1$, we can use the asymptotic form of K_0 for small arguments, such that $2\pi G(|\mathbf{x}|)\approx-\ln(\gamma_e|\mathbf{x}|/2\lambda_c)$. Here, $\gamma_e\approx 1.78\,1972$ is the Euler-Mascheroni constant exponentiated.

We introduce auxiliary multipole moments as the Fourier transforms of the auxiliary fields ψ_i on the contact line circles $\partial S_{i,\text{ref}}$,

$$\hat{\psi}_{im}=\frac{r_0}{2\pi}\int_0^{2\pi}d\varphi_i e^{im\varphi_i}\psi_i(\mathbf{x}_i(\varphi_i)). \tag{17}$$

The analogous multipole decomposition for the Greens function $G(|\mathbf{x}_i-\mathbf{x}_j|)$ is calculated in Appendix B. Using it, the double integral in the exponent of Eq. (16) can be written as a double sum over the Fourier components, consisting of a self-energy part

$$G_{\text{self}}=\sum_i\int_{\partial S_{i,\text{ref}}}d\ell_i\int_{\partial S_{i,\text{ref}}}d\ell_i\psi_i(\mathbf{x}_i)G(|\mathbf{x}_i-\mathbf{x}_i|)\psi_i(\mathbf{x}_i)=\sum_i\left(-2\pi\ln\left(\frac{\gamma_e r_0}{2\lambda_c}\right)|\hat{\psi}_{i0}|^2+\sum_{n>0}\frac{2\pi}{n}|\hat{\psi}_{in}|^2\right) \tag{18}$$

and an interaction part

$$G_{\text{int}}=2\int_{\partial S_{1,\text{ref}}}d\ell_1\int_{\partial S_{2,\text{ref}}}d\ell_2\psi_1(\mathbf{x}_1)G(|\mathbf{x}_1-\mathbf{x}_2|)\psi_2(\mathbf{x}_2)=2\pi\left[-2\ln\left(\frac{\gamma_e d}{2\lambda_c}\right)\hat{\psi}_{10}\hat{\psi}_{20}+\sum_{\substack{m,n=0\\ m+n\geq 1}}\frac{(-1)^n}{m+n}\binom{m+n}{n}\times\left(\frac{r_0}{d}\right)^{m+n}(\hat{\psi}_{1m}\hat{\psi}_{2n}+\hat{\psi}_{1-m}\hat{\psi}_{2-n})\right]. \tag{19}$$

Inserting these expressions into Eq. (16), the functional integral over the auxiliary fields can be written as an integral over their multipole moments. The partition function then reads

$$Z_{\mathrm{fluc}} = \int \prod_{i=1}^{2} \mathcal{D}\psi_i \exp\left[-\frac{k_B T}{2\gamma} \begin{pmatrix} \hat{\boldsymbol{\Psi}}_1 \\ \hat{\boldsymbol{\Psi}}_2 \end{pmatrix}^{\mathrm{T}} \begin{pmatrix} \hat{\mathbf{G}}_{\mathrm{self}} & \hat{\mathbf{G}}_{\mathrm{int}} \\ \hat{\mathbf{G}}_{\mathrm{int}} & \hat{\mathbf{G}}_{\mathrm{self}} \end{pmatrix} \times \begin{pmatrix} \hat{\boldsymbol{\Psi}}_1 \\ \hat{\boldsymbol{\Psi}}_2 \end{pmatrix} \right], \tag{20}$$

where the vectors $\hat{\boldsymbol{\Psi}}_i = (\hat{\psi}_{i0}, \hat{\psi}_{i1}, \hat{\psi}_{i-1}, \ldots)$ contain the auxiliary multipole moments of colloid i. The coupling matrix $\hat{\mathbf{G}}$ which contains the Fourier modes of the Green's function $G(\mathbf{x}_i - \mathbf{x}_j)$ has a block structure. The self-energy submatrices $\hat{\mathbf{G}}_{\mathrm{self}}$ that describe the coupling between auxiliary moments of the same colloid are diagonal, and their elements can be read off Eq. (18). The off-diagonal blocks $\hat{\mathbf{G}}_{\mathrm{int}}$ characterize the interaction between the multipole moments residing on different colloids and are assigned by Eq. (19). Note that all matrix element coupling modes with positive and negative m vanish. From Eq. (20) we find that the fluctuation part of the free energy reads

$$\mathcal{F}_{\mathrm{fluc}} = -k_B T \ln Z_{\mathrm{fluc}} \propto k_B T \ln \det \hat{\mathbf{G}}, \tag{21}$$

where in principle the matrix $\hat{\mathbf{G}}$ is infinite dimensional and divergent and therefore requires regularization. However, after performing the logarithm to calculate the free energy these divergencies only reside in terms independent of the geometrical arrangement of the two colloids, and therefore the derivative of the logarithm with respect to d which corresponds to the Casimir force is finite. Hence, the physically important properties of $\mathcal{Z}_{\mathrm{fluc}}$ reside in the off-diagonal blocks of the matrix $\mathbf{G}$ which describe the interaction between the colloids depending on their separation d, whereas the self-energy part ensures the correct normalization of the interaction. Equation (19) allows for a systematic expansion of the logarithm in Eq. (21) in powers of r_0/d,

$$\mathcal{F}_{\mathrm{fluc}}(d) = \frac{k_B T}{2} \sum_n f_{2n}^{\mathrm{fluc}} \left(\frac{r_0}{d} \right)^{2n}, \tag{22}$$

where the coefficients f_{2n}^{fluc} depend on the logarithms $-\ln(\gamma_e d/2\lambda_c)$ and $-\ln(\gamma_e r_0/2\lambda_c)$. The number of auxiliary multipoles included in the calculation of the asymptotic form of $\mathcal{F}_{\mathrm{fluc}}$ in Eq. (22) is determined by the desired order in r_0/d. The individual contributions in this expansion can be understood as (possibly higher-order) auxiliary multipole-multipole interactions, related to specific products of the matrix elements of $\mathbf{G}$. So, e.g., all the logarithmic contributions to the coefficients in Eq. (22) are related to interactions of the auxiliary monopoles. Note that we cannot perform $\lim_{\lambda_c \to \infty} f_{2n}^{\mathrm{fluc}}$ because of the logarithmic contributions mentioned above. These logarithmic divergencies are reminiscent of the long-range correlations of the capillary waves which lead to a width of the free interface which diverges logarithmically with λ_c or with the system size if gravity is absent. For the Casimir force itself, however, we find a finite value in the limit $\lambda_c \to \infty$. In the asymptotic range $r_0/d \ll 1$ and in the limit $\lambda_c/d \to \infty$ the leading term of the fluctuation force is governed by the first term in the series Eq. (22), f_0^{fluc}, and reads

$$F_{\mathrm{fluc}} = k_B T \frac{\partial}{\partial d} \ln \mathcal{Z}_{\mathrm{fluc}} \to -\frac{k_B T}{2} \frac{1}{d \ln(d/r_0)} + O(d^{-3}),$$

$$\frac{d}{r_0} \gg 1, \quad \frac{d}{\lambda_c} \to 0. \tag{23}$$

Note, however, that the limit $\lambda_c \to \infty$ here is slowly converging with a leading correction term of the order $1/(d \ln \lambda_c)$,

$$-\frac{\partial f_0^{\mathrm{fluc}}}{\partial d} \xrightarrow{d/\lambda_c \ll 1} -\frac{1}{2} \frac{1}{d \ln(d/r_0)} \left(1 + \frac{\ln(r_0/d)}{2 \ln(r_0/\lambda_c)} + O((\ln(r_0/d)^2 / \ln(r_0/\lambda_c)^2) \right) \tag{24}$$

and that the free energy difference corresponding to Eq. (23), $\mathcal{F}(d) \sim \ln \ln(r_0/d)$, is actually ill defined, because the effective colloidal interaction in case (B1)-(B1)—fixed colloids and pinned interface—is only meaningful for a finite capillary length λ_c.

B. Mean-field part

The calculation of $\mathcal{Z}_{\mathrm{mf}}$ [Eq. (10)] requires the solution of the Euler-Lagrange equation (9), $(-\Delta + \lambda_c^{-2}) u_{\mathrm{mf}}(\mathbf{x}) = 0$ for $\mathbf{x} \in \mathbb{R}^2 \setminus \cup_i S_{i,\mathrm{ref}}$ and the (fluctuating) boundary conditions

$$u_{\mathrm{mf}}(\mathbf{x}_i) = f_i(\mathbf{x}_i) \tag{25}$$

with $\mathbf{x}_i \in \partial S_{i,\mathrm{ref}}$ and $u_{\mathrm{mf}}(\mathbf{x}) \to 0$ for $|\mathbf{x}| \to \infty$. In fact a solution to a similar problem (with Neumann boundary conditions) was given in Ref. [27] in terms of bipolar coordinates which, however, is involved if applied to the general Dirichlet boundary conditions in our case. For our purpose it is more convenient to write the solution as a superposition

$$u_{\mathrm{mf}}(\mathbf{x}) = u_1(\mathbf{x} - \mathbf{r}_1) + u_2(\mathbf{x} - \mathbf{r}_2) \equiv u_1(r_1, \varphi_1) + u_2(r_2, \varphi_2), \tag{26}$$

where $\mathbf{r}_i$ is the center position of circle $S_{i,\mathrm{ref}}$. The general solutions u_i of the mean-field equation (9) in polar coordinates (r_i, φ_i) with respect to the centers of the reference contact line circles $S_{i,\mathrm{ref}}$ (see Fig. 2) can be written as linear combinations

$$u_i(r_i, \varphi_i) = \sum_m A_{im} a_{im}(r_i, \varphi_i). \tag{27}$$

The functions a_{im} are defined by

$$a_{i0}(r_i, \varphi_i) = \frac{K_0(r_i/\lambda_c)}{K_0(r_0/\lambda_c)} \approx \frac{\ln(\gamma_e r_i/2\lambda_c)}{\ln(\gamma_e r_0/2\lambda_c)},$$

$$a_{im}(r_i, \varphi_i) = \frac{K_m(r_i/\lambda_c)}{K_m(r_0/\lambda_c)} e^{im\varphi_i} \approx \left(\frac{r_0}{r_i} \right)^{|m|} e^{im\varphi_i}, \tag{28}$$

which are normalized for convenience and where we have used the asymptotic form of the modified Bessel functions K_m for small arguments $r_i/\lambda_c \ll 1$. As the solution has to match the boundary conditions at both circles $\partial S_{1,\mathrm{ref}}$ and $\partial S_{2,\mathrm{ref}}$, we project u_{mf} onto the complete set of functions on

$\partial S_{1,\mathrm{ref}}$, $e^{im\varphi_1}$ and on $\partial S_{2,\mathrm{ref}}$, $e^{im\varphi_2}$, respectively. The expansion coefficients of these projections of u_{mf} must equal the boundary multipole moments at the corresponding circle which leads to a system of linear equations for the expansion coefficients $\{A_{im}, B_{im}\}$ of the u_i,

$$A_{1m} + \sum_{n=-n_{\max}}^{n_{\max}} a_{1,mn} A_{2n} = P_{1m},$$

$$A_{2m} + \sum_{n=-n_{\max}}^{n_{\max}} a_{2,mn} A_{1n} = P_{2m}. \tag{29}$$

In Eq. (29), the matrix coefficients $a_{1,mn}$ are given by the projection coefficients

$$a_{1,mn} = \frac{1}{2\pi} \int_0^{2\pi} d\varphi_1 e^{im\varphi_1} a_{2n}(r_2, \varphi_2), \tag{30}$$

and analogously $a_{2,mn}$ is given in terms of the projection of $a_{1m}(r_1, \varphi_1)$ onto $e^{im\varphi_2}$. In Eq. (29), we have truncated the Fourier expansions at a maximum order $n_{\max}$. Indeed, the numerical solution shows rapid convergence of the expansions in Eq. (27) in the whole range of colloid-colloid separations d, such that they can be truncated at $n_{\max} \approx 20$. Through the inversion of the linear system (29) the coefficients A_{im} and B_{im} can be expressed as linear combinations of the boundary multipoles,

$$A_{im} = \sum_{j=1}^{2} \sum_{n=-n_{\max}}^{n_{\max}} p_{imjn} P_{jn}. \tag{31}$$

Using the asymptotic forms of the functions a_{im} given in Eq. (28), expressing $r_2 = r_2(d, r_1, \varphi_1)$ and $\varphi_2 = \varphi_2(d, r_1, \varphi_1)$ by the polar coordinates with respect to circle $S_{1,\mathrm{ref}}$ and vice versa for circle $S_{2,\mathrm{ref}}$, and expanding the projection coefficients $a_{i,mn}$ in Eq. (29) in r_0/d, the coefficients p_{imjn} in Eq. (31) can be written as a power series in r_0/d. Inserting the solution (26) with the expression (31) for the A_{im} into the line integrals for the mean-field energy $\mathcal{H}[u_{\mathrm{mf}}]$ in the exponent of Eq. (10), we can write $\mathcal{H}[u_{\mathrm{mf}}]$ as a quadratic form of the boundary multipole moments P_{im}, described by a matrix $\mathbf{E}$ with block structure,

$$\mathcal{H}_{\mathrm{mf}} = -\frac{\gamma r_0}{2} \sum_i \int_0^{2\pi} d\varphi_i f_i(\varphi_i) \frac{\partial u_{\mathrm{mf}}(\mathbf{x}(\varphi_i))}{\partial r_i} + \sum_i \mathcal{H}_{\mathrm{b},i}[f_i, h_i]$$
$$= \frac{\gamma}{2} \begin{pmatrix} \hat{\mathbf{f}}_1 \\ \hat{\mathbf{f}}_2 \end{pmatrix}^{\mathrm{T}} \begin{pmatrix} \mathbf{E}_{1\mathrm{self}} & \mathbf{E}_{\mathrm{int}} \\ \mathbf{E}_{\mathrm{int}} & \mathbf{E}_{2\mathrm{self}} \end{pmatrix} \begin{pmatrix} \hat{\mathbf{f}}_1 \\ \hat{\mathbf{f}}_2 \end{pmatrix} + \pi\gamma \sum_i (P_{i0} - h_i)^2. \tag{32}$$

Here, the submatrices $\mathbf{E}_{i,\mathrm{self}}$ and $\mathbf{E}_{\mathrm{int}}$ describe the coupling energy of the multipole moments of the same contact line f_i and from different contact lines, respectivly, and their elements are given by

$$E^{mn}_{i,\mathrm{self}} = 2\pi\delta_{mn}(1 - \delta_{m0}) - \int_0^{2\pi} r_0 d\varphi_i e^{im\varphi_i} \sum_k p_{ikin} \frac{\partial}{\partial r_i} a_{ik}(r_i, \varphi_i), \tag{33}$$

$$E^{mn}_{12,\mathrm{int}} = -\int_0^{2\pi} r_0 d\varphi_1 e^{im\varphi_1} \sum_k p_{2k1n} \frac{\partial}{\partial r_1} a_{2k}[r_2(\varphi_1), \varphi_2(\varphi_1)], \tag{34}$$

and analogously for $E^{mn}_{21,\mathrm{int}}$. Applying again the expansions of the functions a_{ik} in powers of r_0/d in the expression for $E^{mn}_{12,\mathrm{int}}$ and using the series expressions for the coefficients p_{imjn}, the matrix elements can be written as a power series in r_0/d in the asymptotic range $r_0 \ll d \ll \lambda_c$. The mean-field part of the partition sum Eq. (10) can then be written as

$$\mathcal{Z}_{\mathrm{mf}} = \int \prod_i \mathcal{D}f_i \exp\left(-\frac{\mathcal{H}_{\mathrm{mf}}}{k_{\mathrm{B}}T}\right) \tag{35}$$

such that the d-dependent part of $\mathcal{Z}_{\mathrm{mf}}$ is proportional to $\det \mathbf{E}$. As discussed in Sec. II A, the functional measure is given by a product $\mathcal{D}f_i = dh_i \Pi_{m=-M}^{M} dP_{im}$, where M depends on the chosen model for the boundary condition at the contact line. Inserting the power series of the matrix elements $E^{mn}_{i,\mathrm{int}}$ and $E^{mn}_{i,\mathrm{self}}$ and expanding the free energy $\mathcal{F}_{\mathrm{mf}}(d) \propto k_{\mathrm{B}}T \ln \det \mathbf{E}$, we arrive at a series similar in form to the fluctuation part, Eq. (22),

$$\mathcal{F}_{\mathrm{mf}}(d) = \frac{k_{\mathrm{B}}T}{2} \sum_n f^{\mathrm{mf}}_{2n} \left(\frac{r_0}{d}\right)^{2n}, \tag{36}$$

where again the coefficients f^{mf}_{2n} are functions of the monopole self-energy and interaction coupling elements, $-\ln(\gamma_{\mathrm{e}} r_0/2\lambda_c)$ and $-\ln(\gamma_{\mathrm{e}} d/2\lambda_c)$, respectively. Before discussing the analytic structure of the dependence on d, we remind the reader that the integration measure $\mathcal{D}f_i$ differs between the cases (A)—no pinning, (B2)—pinning and height fluctuation of the colloids, and (B3)—pinning with collective height and tilt fluctuations of the contact line.

In all cases for the boundary conditions except (B1)-(B1) we have a mean-field contribution, and the leading term of the free energy in the long-range regime $d \gg r_0$ (with $\lambda_c \to \infty$) is determined by the boundary monopole-monopole interaction and leads to a repulsive effective force between the colloids,

$$F_{\mathrm{mf}} = k_{\mathrm{B}}T \frac{\partial}{\partial d} \ln \mathcal{Z}_{\mathrm{mf}} \to \frac{k_{\mathrm{B}}T}{2} \frac{1}{d \ln(d/r_0)} + O(d^{-3}),$$

$$\frac{d}{r_0} \gg 1, \quad \frac{d}{\lambda_c} \to 0, \tag{37}$$

which is equal in size but opposite in sign to the fluctuation contributions, and thus these terms cancel. Depending on the precise type of the boundary conditions, we find $f^{\mathrm{mf}}_{2n} = -f^{\mathrm{fluc}}_{2n}$ up to a certain order n, such that the attractive force contributions from the fluctuation part are cancelled by a repulsive one from the mean-field part. The resulting leading order of the effective force can be inferred from Table I.

C. Kardar's method

Here we calculate the partition function directly without splitting the fluctuating field u into a mean-field and a fluctuation part. The starting point is Eq. (14) from Sec. II C The δ functions can again be expressed by auxiliary fields ψ_i, now defined on the two-dimensional circular domains $S_{i,\mathrm{ref}}$ as opposed to the auxiliary fields of Sec. III A which are defined on the one-dimensional circles $\partial S_{i,\mathrm{ref}}$:

$$\mathcal{Z} = \int \mathcal{D}u \int \prod_{i=1}^{2} \mathcal{D}\psi_i \int \mathcal{D}f_i \exp\left(- \frac{\mathcal{H}_{\mathrm{tot}}[f_i,u]}{k_{\mathrm{B}}T} + i \int_{S_i,\mathrm{ref}} d^2x\, \psi_i(\mathbf{x})[u(\mathbf{x}) - f_{i,\mathrm{ext}}(\mathbf{x})] \right). \tag{38}$$

The functions $f_{i,\mathrm{ext}}$ which describe the interface extension to $S_{i,\mathrm{ref}}$ have been defined in Eq. (11) in terms of a multipole expansion in the P_{im}. The total Hamiltonian contains the capillary wave Hamiltonian and the boundary and correction terms (see Sec. II C) and reads

$$\mathcal{H}_{\mathrm{tot}} = \frac{\gamma}{2} \int_{\mathbb{R}^2} d^2x \left((\nabla u)^2 + \frac{u^2}{\lambda_c^2} \right) + \frac{\pi\gamma}{2} \sum_i \left(2(P_{i0} - h_i)^2 + 4 \sum_{|m|\geqslant 1} (1 - |m|)|P_{im}|^2 \right). \tag{39}$$

Similarly to the evaluation of the fluctuation part, Sec. III A, we introduce multipole moments Ψ_{im} of the auxiliary fields by inserting unity into $\mathcal{Z}$, Eq. (38):

$$1 = \int \prod_{i=1}^{2} \prod_m d\Psi_{im}\, \delta\left(\Psi_{im} - \int_{S_i} d^2x (r/r_0)^{|m|} e^{-im\varphi} \psi(\mathbf{x}) \right). \tag{40}$$

In contrast to the evaluation of the fluctuation term in Sec. III A, there will be constraints on the lowest multipoles which contribute to $\mathcal{Z}$. To see this we note that, after shifting $h_i \to h_i - P_{i0}$, the Hamiltonian $\mathcal{H}_{\mathrm{tot}}$ no longer depends on the boundary monopole moments P_{i0} and the dipole moments P_{i1} and the only dependence of $\mathcal{Z}$ on these moments is through the constraint function $f_{i,\mathrm{ext}}$. Recalling the definition of the integration measure $\mathcal{D}f_i$ for the various boundary conditions, Sec. II A and performing the integration over P_{i0} and P_{i1} where applicable, we immediately find

$$\mathcal{Z} \sim \begin{cases} \displaystyle\int \prod_{i=1}^{2} \prod_m d\Psi_{im} \cdots \delta(\Psi_{i0}) \cdots, & \text{case (B2)}, \\ \displaystyle\int \prod_{i=1}^{2} \prod_m d\Psi_{im} \cdots \delta(\Psi_{i0}) \delta(\Psi_{i-1}) \delta(\Psi_{i1}) \cdots & \text{cases (A) and (B3)}. \end{cases} \tag{41}$$

Having noticed these constraints on the auxiliary fields, we proceed by integrating over the field u in Eq. (38):

$$\mathcal{Z} = \int \prod_{i=1}^{2} \mathcal{D}\psi_i \int \mathcal{D}f_i \exp\left[- \frac{k_{\mathrm{B}}T}{2\gamma} \sum_{i,j=1}^{2} \int_{S_{i,\mathrm{ref}}} d^2x_i \times \int_{S_{j,\mathrm{ref}}} d^2x_j \psi_i(\mathbf{x}_i) G(|\mathbf{x}_i - \mathbf{x}_j|) \psi_j(\mathbf{x}_j) - \frac{\pi\gamma}{2k_{\mathrm{B}}T} \left(2(P_{i0} - h_i)^2 + 4 \sum_{|m|\geqslant 1} (1 - |m|)|P_{im}|^2 \right) - i \sum_{i=1}^{2} \int_{S_{i,\mathrm{ref}}} d^2x\, \psi(\mathbf{x}) f_{i,\mathrm{ext}}(\mathbf{x}) \right], \tag{42}$$

where—as in Eq (16)—G is the Green's function of the capillary wave Hamiltonian. A somewhat longer calculation shows that $\mathcal{Z}$ can be split into into an interaction part (coupling the auxiliary multipole moments Ψ_{im} for different colloid labels i), a self-energy part (depending on Ψ_{im} for each value of i separately), and a remainder (the sum of the boundary and correction Hamiltonians):

$$\mathcal{Z} = \int \prod_{i=1}^{2} \prod_m d\Psi_{im} \int \mathcal{D}f_i \times \exp\left\{ - \frac{k_{\mathrm{B}}T}{2\gamma} (\mathcal{H}_{\mathrm{int}}[\Psi_{1m}, \Psi_{2m}] + \mathcal{H}_{i,\mathrm{self}}[\Psi_{im}]) \right\} \times \exp\left[- \frac{\pi\gamma}{2k_{\mathrm{B}}T} \left(2(P_{i0} - h_i)^2 + \sum_{|m|\geqslant 1} (1 - |m|)|P_{im}|^2 \right) - i \sum_m \Psi_{im} P_{im} \right]. \tag{43}$$

The interaction part

$$\mathcal{H}_{\rm int} = 2\int_{S_{1,\rm ref}} d^2x_1 \int_{S_{2,\rm ref}} d^2x_2 \psi_1(\mathbf{x}_1) G(|\mathbf{x}_1-\mathbf{x}_2|)\psi_2(\mathbf{x}_2)$$
$$= \frac{1}{2\pi}\Bigg[-2\ln\left(\frac{\gamma_e d}{2\lambda_c}\right)\Psi_{10}\Psi_{20} + \sum_{\substack{l_1,l_2=0\\ l_1+l_2\geqslant 0}} \frac{(-1)^{l_2}}{l_1+l_2}\binom{l_1+l_2}{l_2} \times\left(\frac{r_0}{d}\right)^{l_1+l_2}(\Psi_{1l_1}\Psi_{2l_2}+\Psi_{1-l_1}\Psi_{2-l_2})\Bigg] \quad (44)$$

is a bilinear form in the auxiliary multipole moments; it was derived using the multipole expansion of the Green's function $G(|\mathbf{x}_1-\mathbf{x}_2|)\simeq -\ln(\gamma_e|\mathbf{x}_1-\mathbf{x}_2|/2\lambda_c)$ (valid for $d\gg r_0$) which is presented in Appendix B in more detail. The self-energy part

$$\exp\left(-\frac{k_BT}{2\gamma}\mathcal{H}_{i,\rm self}\right) = \int\prod_{i=1}^{2}\mathcal{D}\psi_i\,\delta\left(\Psi_{im}-\int_{S_i} d^2x (r/r_0)^{|m|}e^{-im\varphi}\psi_i(\mathbf{x})\right) \times\exp\left(-\frac{k_BT}{2\gamma}\int_{S_i}d^2x\int_{S_i}d^2x'\,\psi_i(\mathbf{x})G(|\mathbf{x}-\mathbf{x}'|)\psi_i(\mathbf{x})\right) \times\exp\left(-i\int_{S_{i,\rm ref}} d^2x\;\psi_i(\mathbf{x})f_{i,\rm ext}(\mathbf{x})+i\sum_m \Psi_{im}P_{im}\right) \quad (45)$$

is evaluated in Appendix C, with the result

$$\mathcal{H}_{i,\rm self} = -|\Psi_{i0}|^2\frac{\ln(\gamma_e r_0/2\lambda_c)}{2\pi}+\sum_{m>0}\frac{|\Psi_{im}|^2}{2\pi|m|}. \quad (46)$$

Combining Eqs. (43), (44), and (46), the partition function can be written as

$$Z=\int\prod_{i=1}^{2}\prod_m \mathcal{D}\Psi_{im}\mathcal{D}f_i \times\exp\left[-\frac{k_BT}{2\gamma}\begin{pmatrix}\boldsymbol{\Psi}_1\\ \boldsymbol{\Psi}_2\end{pmatrix}^{\dagger}\begin{pmatrix}\hat{\mathbf{H}}_{\rm self} & \hat{\mathbf{H}}_{\rm int}\\ \hat{\mathbf{H}}_{\rm int} & \hat{\mathbf{H}}_{\rm self}\end{pmatrix}\begin{pmatrix}\boldsymbol{\Psi}_1\\ \boldsymbol{\Psi}_2\end{pmatrix}\right], \quad (47)$$

where the vectors $\boldsymbol{\Psi}_i=(\Psi_{i0},P_{i0},\Psi_{i1},P_{i1},\Psi_{i-1},P_{i-1},\ldots)$—in contrast to $\hat{\boldsymbol{\Psi}}_i$ in Sec. III A—contain all involved auxiliary and boundary multipole moments. The elements of the matrix $\mathbf{H}$ describe the coupling of these multipole moments, where the self-energy block couples multipoles defined on the same circles $S_{i,\rm ref}$. The self-energy matrix $\hat{\mathbf{H}}_{\rm self}$ can be read off Eqs. (43) and (46). The elements of the interaction matrix $\hat{\mathbf{H}}_{\rm int}$ are determined by the interaction energy $\mathcal{H}_{\rm int}$ in Eq. (44) and couple the auxiliary multipole moments of different colloids. All matrix elements representing couplings of other multipoles are zero.

As in Eqs. (20) and (35), the exponent in Eq. (47) is a bilinear form; however, here it is combined for all types, boundary multipole moments P_{im}, and auxiliary multipoles Ψ_{im}. The computation of the partition function amounts to the calculation of $\det\hat{\mathbf{H}}$. Expanding the logarithm of this determinant for $r_0/d\ll 1$, and taking the derivative with respect to d, we directly obtain the asymptotic form Eq. (15) for the total Casimir force,

$$F(d)=-\frac{k_BT}{2}\frac{\partial}{\partial d}\sum_n f_{2n}^{\rm Kardar}\left(\frac{r_0}{d}\right)^{2n} \quad (48)$$

with $f_{2n}^{\rm Kardar}=f_{2n}^{\rm fluc}+f_{2n}^{\rm mf}$ as it should be.

In contrast to the calculation before, the different leading power laws for the different cases (A) and (B1)–(B3) can be understood easily. As described in the beginning of this section, the cancellation of leading terms in the free energy arises as a consequence of the vanishing of certain auxiliary multipole moments of the auxiliary fields defined on $S_{i,\rm ref}$. The leading terms of the Casimir force are determined by the interaction of the lowest nonvanishing auxiliary multipoles. Note, however, that the auxiliary monopoles [which are nonzero only in case (B1)] lead to logarithmic terms in the interaction which vanish (logarithmically) for mixed boundary conditions in the limit $r_0/\lambda_c\to 0$, such that in these cases the Casimir force is determined by the next higher multipole interaction (cf. Table I). We remind the reader that the constraints of vanishing auxiliary monopole and dipole moments result from the independence of $\mathcal{H}_{\rm tot}$ of the boundary monopole and dipole moments and that this is only captured correctly by the inclusion of the correction Hamiltonian $\mathcal{H}_{\rm corr}$ (see Sec. II C).

At this point we insert the following observation: If the sum of boundary and correction Hamiltonians were zero, all multipole moments Ψ_{im} would be zero and consequently all coefficients in the expansion of the Casimir force in terms of r_0/d would vanish—i.e., the total Casimir force would be zero. This happens for the boundary Hamiltonian [28]

$$\mathcal{H}_{{\rm b},i}=2\pi\gamma\sum_{m\geqslant 1} m|P_{im}|^2 \quad (49)$$

$$=\frac{\gamma}{16\pi}\int_{\partial S_{i,\rm ref}}d\phi\int_{\partial S_{i,\rm ref}}d\phi'\,\frac{[f_i(\phi)-f_i(\phi')]^2}{\sin^2\left[\frac{1}{2}(\phi-\phi')\right]}. \quad (50)$$

Thus we see that the boundary Hamiltonian needs to be of nonlocal nature in the contact line height f_i to make the Casimir force vanish.

IV. SHORT-RANGE BEHAVIOR

A. Fluctuation part

In the opposite limit of small surface-to-surface distance $h=d-2r_0\ll r_0$ the fluctuation force can be calculated by using the Derjaguin (or proximity) approximation [29]. It consists in replacing the local force density on the contact lines by the result for the fluctuation force per length $f_{2\rm d}(\tilde{h})$ between two parallel lines with a separation distance $\tilde{h}$ and integrating over the two opposite contact line half circles to obtain the total effective force between the colloids.

The Casimir force between two parallel surfaces was calculated in Ref. [30] in a general approach and explicitly for

three-dimensional problems. Applied to two dimensions we obtain $f_{2d}(\tilde{h})=-k_BT\pi/(24\tilde{h}^2)$. Integrating over the opposing contact line half circles yields

$$F_{\text{fluc}} \approx -2\frac{\pi k_B T}{24}\int_0^{r_0} dy \frac{1}{(h+2r_0-2\sqrt{r_0^2-y^2})^2} \xrightarrow{r_0/h\to\infty} -k_B T\frac{\pi^2}{48}\frac{r_0^{1/2}}{h^{3/2}}+O(h^{-1/2}). \quad (51)$$

for the dominant contribution to the Casimir force from the fluctuation part in the limit $h/r_0 \ll 1$. Note, that this strong increase as $h\to 0$ is a consequence of the finite (mesoscopic) size of the colloids and is missed if the colloids are approximated by pointlike objects [31].

B. Mean-field part

Here, we exemplify the asymptotic behavior of the mean-field force for close colloid separations $h\to 0$ by case (B2) for the boundary conditions where only fluctuations of the boundary monopoles occur. From the numerical results (see next section) we observe that the type of divergence of the mean-field force as $h\to 0$ is obtained correctly by considering only monopole fluctuations; including higher multipole moments affects the force only by a multiplicative constant. (This is in marked contrast to the long-range regime.)

In order to apply the Derjaguin approximation, we calculate the mean field between two parallel lines $\partial S_{1/2}$ on which the field is pinned to a fluctuating value $u_{\text{mf}}(\partial S_i)=P_{i0}$ (corresponding to monopole boundary conditions). The mean-field energy $\mathcal{H}_{\text{mf}}$ in Eq. (32) is represented by a 2×2 matrix $\mathbf{E}$. By diagonalizing $\mathbf{E}$ we can write $\mathcal{H}_{\text{mf}}=(\gamma L_y/2)[e_s Z^2+e_a(\Delta z^2)]$, where e_s and e_a are the eigenvalues of $\mathbf{E}$, and $Z=P_{10}+P_{20}$ and $\Delta z=P_{10}-P_{20}$ are the symmetric and the antisymmetric superposition of u_{mf} at the boundaries ∂S_i, respectively. L_y is the length of the boundary lines. In fact, the line densities e_s and e_a correspond up to a factor to the mean-field energies of the solutions of the mean-field equation (25) with symmetric $(u_s|\partial_{S_{1/2}}=Z)$ and antisymmetric $(u_a|\partial_{S_{1/2}}=\pm\Delta z)$ boundary conditions, respectively, and the general mean-field solution is given by by $u_{\text{mf}}=(u_s+u_a)/2$. For $\lambda_c\to\infty$ the mean-field equation reduces to the Laplace equation $\Delta u_{\text{mf}}=0$ between parallel lines which are in the x direction a distance $\tilde{h}$ apart. The antisymmetric and symmetric solutions read $u_a=(2\Delta z/\tilde{h})x$ and $u_s=\text{const}$, respectively, with the corresponding line densities $e_s=0$ and $e_a=4/\tilde{h}$. A vanishing e_s signifies that a collective vertical shift of the interface does not cost any energy. This leads to the divergence of the integral over Z in the partition function Z_{mf}, which physically is not interesting and can be neglected. Applying the Derjaguin approximation [similar to Eq. (51)] to only the antisymmetric mode yields the corresponding energy E_a for the two circles a distance h apart:

$$E_a \approx -2\gamma\int_0^{r_0} dy \frac{2(\Delta z)^2}{h+2r_0-2\sqrt{r_0^2-y^2}} \approx 2\pi\gamma(\Delta z)^2\sqrt{\frac{r_0}{h}} + O(1). \quad (52)$$

Thus the h-dependent mean-field part of the free energy reads $\mathcal{F}_{\text{mf}}\simeq -k_BT\ln\int d(\Delta z)\exp(-E_a/k_BT)=-(k_BT/4)\ln(h/r_0)+\text{const}$. So, in the limit $h=d-2R\to 0$, the leading (divergent) part of the effective mean-field force F_{mf} is repulsive and reads

$$F_{\text{mf}}(h\to 0)\approx \frac{k_BT}{4h}. \quad (53)$$

It appears physically less obvious why the Derjaguin approximation could also be applied to higher boundary multipole moments n, especially if $h\lesssim R/n$. If one nevertheless does so one finds that in this regime $h\lesssim R/n$ the mean-field force diverges more slowly than $1/h$ whereas for $h\ll R/n$ the monopole behavior is recovered. This is in accordance with our numerical results. Note that this holds true also for different types of boundary conditions on the two colloids.

V. INTERMEDIATE DISTANCES: NUMERICAL CALCULATION

For intermediate distances $d\simeq r_0$ the fluctuation-induced force has to be calculated numerically. We will do this as in the previous sections for the fluctuation and the mean-field part separately. For the fluctuation part, we shall apply a method which was introduced in Ref. [32]. The starting point is Eq. (16) for the partition function Z_{fluc}. Introducing an equidistant mesh with N points $\varphi_{ij}=(2\pi/N)j$, $0\leq j<N$, on the contact line circles $\partial S_{i,\text{ref}}$ converts the double integral in the exponent to a double sum. Then the functional integrals over the ψ_i are replaced by ordinary Gaussian integrals over the $\psi_i(\mathbf{x}_i(\varphi_{ij}))$, $\mathcal{D}\psi_i\simeq\Pi_{j=0}^{N} d\psi_i(\mathbf{x}_i(\varphi_{ij}))$. In the exponent, the $\psi_i(\mathbf{x}_i(\varphi_{ij}))$ are coupled by a matrix $\mathbf{G}$ with elements $G_{ii'}^{jj'}=G[|\mathbf{x}_i(\varphi_{ij})-\mathbf{x}_{i'}(\varphi_{i'j'})|]$. Performing the Gaussian integrals and disregarding divergent and d-independent terms immediately leads to $\mathcal{F}_{\text{fluc}}=(k_BT/2)\ln\det[\mathbf{G}_\infty^{-1}\mathbf{G}(d)]$ for the fluctuation free energy. Here, $\mathbf{G}_\infty\equiv\lim_{d\to\infty}\mathbf{G}(d)$. It contains the self-energy contributions and is needed for the regularization of the free energy. Deriving with respect to d, the Casimir force can be written as

$$F_{\text{fluc}}(d)=-\frac{k_BT}{2}\text{tr}[\mathbf{G}(d)^{-1}\partial_d\mathbf{G}(d)]. \quad (54)$$

The advantage of the direct calculation of the force is that Eq. (54) does not contain any divergent parts which would require regularization, thus easing the numerical treatment considerably. The determinant is computed by using a standard LU decomposition [33]. We find good convergence of the numerical routine also for small d if $N\approx 5000$, which, however, demands a computation time of about 30 h for each distance point on a standard PC. As discussed in Sec. VI and shown in Fig. 4, we find very good agreement between analytical and numerical results.

The numerical calculation of the mean-field Casimir force can be done very conveniently with the method described in Sec. III B. In order to avoid complex numbers, we used sine and cosine modes instead of Fourier modes for the numerical computations. It is straightforward to rewrite the corresponding equations in Sec. III B by using their real and imaginary

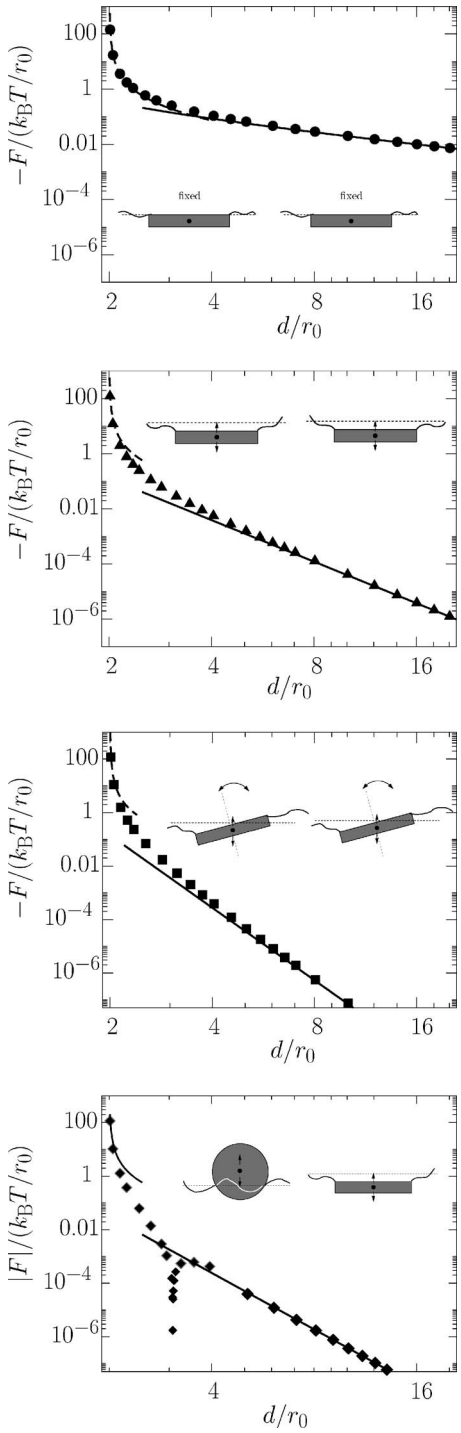

FIG. 4. Comparison of the numerical results for the Casimir force (symbols) with the analytical expressions in the asymptotic ranges of large colloid separations $d \gg r_0$ (full line) and small surface-to-surface distance $h=d-2r_0 \ll r_0$ (dashed line) for various combinations of the boundary condition cases (B1), (B2), (B3), and (A). In the example with mixed boundary conditions, (A)-(B1), we have plotted the absolute value of the force because of the change of sign, which is indicated by a cusp.

parts. Via a numerical evaluation of the integrals for the projection coefficients $a_{i,mn}$ in Eq. (30) and inversion of the linear system Eq. (29) the elements $E^{mn}_{i,\mathrm{self}}$ and $E^{mn}_{12,\mathrm{int}}$ of the matrix $\mathbf{E}$ are computed [see Eqs. (33) and (33)]. Calculating $\ln\det \mathbf{E}$ then provides the free energy $\mathcal{F}_{\mathrm{mf}}$, and the numerical derivative finally the mean-field Casimir force F_{mf}. This scheme turns out to be very efficient and provides results for F_{mf} within seconds. Indeed, the numerical calculations show that it is sufficient to consider $n_{\max} \approx 20$ modes in the expansions of the u_i in Eq. (26) in order to achieve convergence of the results.

A direct numerical implementation of Kardar's method is difficult since the auxiliary fields are defined in this case on $S_{i,\mathrm{ref}}$ which is two dimensional. A discretization of these areas with $N \approx 5000$ points as used for evaluating F_{fluc} would not be sufficient but considerably finer discretizations are forbidding due to memory storage and computing time problems.

VI. DISCUSSION OF RESULTS AND OF POSSIBLE REALIZATIONS

In Fig. 4 we compare numerical results with the analytical expressions for the Casimir force for the long-range asymptotics (Sec. III) and for very small colloid-colloid separations (Sec. IV), respectively.

For all considered combinations for the boundary conditions (B1)–(B3) and (A), we find very good agreement with the analytical predictions in Table I for the long-range regime $d \gtrsim 5r_0$. In the short-range regime, the fluctuation-induced force depends much less on the specific type of boundary conditions at the contact line. In fact, in this regime, the divergence of the fluctuation part force (which applies to all cases), $\sim -h^{-3/2}$, is dominating the total force in this regime and leads to a strong net attraction. As can be seen from the plots in Fig. 4, in case (B1)-(B1) (fixed colloids, no mean-field force) the Derjaguin approximation describes well the numerical data also for intermediate colloid separations $r_0/h=r_0/(d-2r_0) \leqslant 5$. From the plots for the like-boundary cases (B2), (B3), and (A), however, we see that the repulsive contribution from the mean-field part showing a weaker divergence $\sim 1/h$ leads to a strong decrease of the total force for $r_0/h=r_0/(d-2r_0) \geqslant 1$, which, by increasing d, converges to the power laws governing the long-range asymptotics. The rapid decrease of the total force actually renders the Casimir force effectively short-ranged for the like boundary cases (B3) and (A). Note that because of this rapid decay $\sim -1/d^9$, the competing attractive and repulsive contributions from the fluctuation and mean-field part are of almost equal size and our numerical methods which are based on the addition of these quantities are afflicted with numerical uncertanties and are not able to provide reliable results for $d \gtrsim 15r_0$. In the opposite regime of small separations $h=d-2r_0 \ll r_0$, the effect of the boundary conditions is much less pronounced, and the resulting force is dominated by $F_{\mathrm{fluc}} \sim h^{-3/2}$ (attractive) compared with $F_{\mathrm{mf}} \sim h^{-1}$ (repulsive), leading to a strong attractive Casimir interaction in this regime (see Fig. 4). At small distances typically also van der Waals forces become important. They lead to a strong tendency of colloid aggregation, if not compensated by a repulsive interaction. For spherical colloids at small separations and $\theta=\pi/2$ the well-known Derjaguin result for the vdW force reads

$$F_{\mathrm{Derj}}^{\mathrm{vdW}} = -\frac{A_{\mathrm{H}}}{12\pi}\frac{R}{h^2}. \tag{55}$$

Here, the (effective) Hamaker constant A_{H} is determined by the frequency-dependent dielectric permittivities of both the colloids and the two fluid phases. Equation (55) shows an even stronger increase for $h \to 0$. Hence, the vdW force $F_{\mathrm{Derj}}^{\mathrm{vdW}}$ will dominate the Casimir force (51) since the Hamaker constant is typically $A_{\mathrm{H}} \approx (1-10)k_{\mathrm{B}}T$. For smaller Hamaker constants, however, $A_{\mathrm{H}}/k_{\mathrm{B}}T < (\pi^3/4)\sqrt{h/R}$, which in principle can be obtained by refractive index matching between colloids and fluids, we find $|F_{\mathrm{fluc}}| > |F_{\mathrm{Derj}}^{\mathrm{vdW}}|$ and therefore in this distance regime an increased influence of the fluctuation-induced force on particle aggregation. Note, however, that in an experimental realization this constitutes a considerable challenge. For two cylindrical disks with height H the Derjaguin approximation leads to $F_{\mathrm{Derj}}^{\mathrm{vdW}} \sim -(H/h^2)(R/h)^{1/2}$ if $h \ll R, H$. For very thin disks ($H \ll h \ll R$), however, integration over atomic pair potentials $\sim r^{-6}$, which give rise to the vdW force, results in

$$F_{\mathrm{td}}^{\mathrm{vdW}} = -A_{\mathrm{H}}\frac{15\pi^2}{48}\frac{H^2}{h^2}\sqrt{\frac{R}{h}}\frac{1}{h}. \tag{56}$$

In this case, we find $F_{\mathrm{vdW}}/F_{\mathrm{fluc}} = 15(A_{\mathrm{H}}/k_{\mathrm{B}}T)(H/h)^2 \ll 1$, so that for $H \ll h \ll R$ the driving mechanism for flocculation is entirely given by the fluctuation-induced force. Thus, the fluctuation-induced force can strongly enhance the tendency of colloids at interfaces to flocculate. This effect is independent of material parameters, as long as the system is in the capillary wave regime, i.e., for $h \gg \sigma$. For colloid-colloid separations h in the order of the molecular length scale σ of the fluids; however, the capillary wave model is no longer valid. In this regime, the total effective force can be understood by taking into account the formation of a wetting film around the colloids [34] and stays finite.

In experimental realizations, fixing the colloids as required in case (B1) might, e.g., be realized by laser tweezers. In such a setup, the fixing is usually, of course, not ideal, since the vertical movement of the colloid centers is restricted by an external potential of finite width. Including such an external potential for the colloids in our model in fact lowers the repulsive contribution from the mean-field part (as compared to the unfixed case), and therefore leads to an increased long-ranged attractive total Casimir force dominated by the leading term of the fluctuation part, Eq. (23). The extent of this increase is controlled by the strength of the external potential for the colloids, as we will show in the next subsection. However, since laser tweezers act on refractive index gradients, they are not appropriate for particles at the interfaces of colloid-polymer mixtures used in Ref. [36] to produce ultralow-tension surfaces. In this case the external potential has to be provided by another method, like magnetic tweezers or a sterical confinement of the particles caused by parallel plates forming a canal. Then, however, it remains the experimental challenge of separating the fluctuation-induced forces from the direct magnetic interactions between the particles or from possible finite-size effects induced by the canal.

External potential on the colloids

In the effective Hamiltonian introduced in Sec. II we considered only free energy differences resulting from the changes of interfacial areas which are associated with fluctuations around the flat reference configuration. In this subsection we will extend this model to external potentials $V_i(h_i)$ acting on the vertical position h_i of the center of colloid i. We will concentrate on the cases of a constant external force $F_i\mathbf{e}_z$ and a harmonic potential for colloid i, corresponding to $V_i(h_i) = -F_i h_i$ and $V_i(h_i) = \frac{1}{2}D_i(h_i - h_{0,i})^2$, respectively. The vertical forces F_i include, e.g., gravity, whereas the harmonic potential can be realized by a laser tweezer. So this is of particular interest for case (B1) where the colloid positions are fixed.

Then, the total effective Hamiltonian of the two colloids adsorbed at the fluid interface reads

$$\mathcal{H} = \mathcal{H}_{\mathrm{cw}} + \sum_i [\mathcal{H}_{\mathrm{b},i} + V_i(h_i)]. \tag{57}$$

Note that the approximations performed in Sec. II in deriving the capillary wave and boundary Hamiltonian remain valid here if the external force or the displacement of the harmonic potential are small on the scale set by the surface tension, i.e., $F_i \ll 2\pi\gamma r_0$ and $D_i h_0 \ll 2\pi\gamma r_0$, respectively.

The additional external potential has two implications which we will discuss in the following. First, it leads to a deformed equilibrium meniscus as compared to the flat reference interface, which gives rise to a "classical" capillary interaction between the colloids [13]. Second, through the coupling of the colloid position h_i to the interface field u in the boundary Hamiltonian $\mathcal{H}_{\mathrm{b},i}$, the thermal movement of the colloids in the potential V_i can also influence the fluctuation-induced ("nonclassical") force between the colloids.

As described in detail in Ref. [13], the equilibrium meniscus u_{eq} can be found by minimizing the effective Hamiltonian $\mathcal{H}$ with respect to the colloid position h_i and the interface height $u(x,y)$. The equilibrium colloid height $h_{i,\mathrm{eq}}$ is determined from the condition $\partial\mathcal{H}/\partial h_i = 0$ and depends on both the external potential and the mean height of the three-phase contact line on the colloid surfaces. The interface field u_{eq} satisfies the Euler-Lagrange equation (25) of $\mathcal{H}_{\mathrm{cw}}$ with the boundary condition [13]

$$\frac{\partial u_{\mathrm{eq}}(\mathbf{x})}{\partial n_i} = \frac{u_{\mathrm{eq}}(\mathbf{x}) - h_{i,\mathrm{eq}}}{r_0}, \tag{58}$$

where $\partial/\partial n_i$ is the derivative in the outward normal direction of $\partial S_{i,\mathrm{ref}}$. Using the general form of Eqs. (26) and (27) for u_{eq} and projecting the boundary conditions (58) on $\partial S_{i,\mathrm{ref}}$ onto $e^{im\varphi_i}$ as in Sec. III B leads again to a linear system for the expansion coefficients A_{im} similar to Eq. (29).

For a constant external force, we obtain in the asymptotic range $r_0 \ll d \ll \lambda_c$

$$u_{\mathrm{eq}} \simeq -\frac{F_1}{2\pi\gamma}\ln\left(\frac{\gamma_e r_1}{2\lambda_c}\right) - \frac{F_2 r_0}{2\pi\gamma d}\left(\frac{r_0}{r_1}\right)\cos(\varphi_1) - \frac{F_2}{2\pi\gamma}\ln\left(\frac{\gamma_e r_2}{2\lambda_c}\right) - \frac{F_1 r_0}{2\pi\gamma d}\left(\frac{r_0}{r_2}\right)\cos(\varphi_2) \tag{59}$$

for the leading terms in r_0/d of the equilibrium meniscus u_{eq} (see Fig. 2 for the definitions of r_i and φ_i). The capillary interaction arising from the meniscus deformation is given by [13]

$$V_{\mathrm{men}}(d) = \mathcal{H}(d) - \sum_i \mathcal{H}_{i,\infty} \approx \frac{F_1 F_2}{2\pi\gamma}\ln\frac{\gamma_e d}{2\lambda_c} + \frac{F_1^2 + F_2^2}{4\pi\gamma}\left(\frac{r_0}{d}\right)^2. \tag{60}$$

Here, $\mathcal{H}_{i,\infty}$ is the effective energy associated with a single colloid system. The first term in the second line of Eq. (60) is the well-known logarithmic flotation force. Note that in the absence of electrostatic forces the main contribution to the external force usually is gravity which can be neglected for colloid radii $\leqslant 1$ μm as it is much smaller than the thermal energy $k_B T$. The second term describes the leading behavior of the capillary interaction if there is an external force only applied to one of the colloids—and it leads to a repulsive force between the colloids.

For harmonic external potentials the equilibrium meniscus and the capillary interaction potential is calculated in the same way but results in a somewhat lengthy expression for V_{men}. Focusing onto the symmetric case of identical potentials for both colloids, we find that V_{men} vanishes in the limit $\lambda_c \to \infty$: In the absence of gravity a parallel shift of the whole interface does not cost any energy, and, therefore, the response of the system on the presence of the harmonic potentials on the colloids is a shift of the planar interface to a new equilibrium position $u_{\mathrm{eq}} \equiv -h_0 (= h_{0i})$—without a meniscus deformation and, hence, without causing a capillary interaction. The leading term for $1/\lambda_c$ small is given by

$$V_{\mathrm{men}} \simeq \frac{4\pi\gamma h_0^2 \ln(\gamma_e d/2\lambda_c)}{[2\pi\gamma/D - \ln(\gamma_e r_0/2\lambda_c)][2\pi\gamma/D - \ln(\gamma_e r_0 d/4\lambda_c^2)]}. \tag{61}$$

If the minima of the harmonic potentials on the colloids are not identical, we find an additional term

$$V_{\mathrm{men}} \xrightarrow{\lambda_c \to \infty} \frac{\pi\gamma(h_{01} - h_{02})^2}{1 + \pi\gamma(1/D_1 + 1/D_2) + \ln d/r_0} \tag{62}$$

which is not vanishing in the limit $\lambda_c \to \infty$.

The influence of the external potential on the fluctuation-induced force is most conveniently discussed by splitting the interfacial field into an equilibrium and a fluctuation part, $u = u_{\mathrm{eq}} + \Delta u$, similar to the splitting into a mean-field part u_{mf} and a fluctuation part v described in Sec. II B, and analogously $h_i = h_{i,\mathrm{eq}} + \Delta h_i$ for the vertical position of the colloid centers. Note, however, that u_{eq} satisfies the equilibrium boundary conditions (58), whereas u_{mf} is the mean-field part of Δu, i.e., $\Delta u = u_{\mathrm{mf}} + v$, which satisfies the boundary conditions Eq. (3) corresponding to thermal fluctuations of the contact line around its equilibrium position. Inserting this decomposition of the interfacial field u into the extended Hamiltonian Eq. (57) and performing some conversions of the integrals by exploiting Eqs. (25) and (58) together with Gauss's theorem, we find a quite distinct behavior for the cases of a constant external force and of a harmonic potential. In the first case we can rewrite the effective Hamiltonian in the form $\mathcal{H}[u_{\mathrm{eq}} + \Delta u] = \mathcal{H}[u_{\mathrm{eq}}] + \mathcal{H}_{\mathrm{cw}}[\Delta u] + \mathcal{H}_{\mathrm{b}}[\Delta u, \Delta h_i]$. That means that the effective Hamiltonian relevant for the fluctuation-induced force is independent of the external force in this case. The only effect of a constant external force, hence, is the deformation of the equilibrium meniscus which leads to the *classical* interaction described by Eq. (60). In the case of a harmonic external potential, however, we find $\mathcal{H}[u_{\mathrm{eq}} + \Delta u] = \mathcal{H}[u_{\mathrm{eq}}] + \mathcal{H}_{\mathrm{cw}}[\Delta u] + \mathcal{H}_{\mathrm{b}}[\Delta u, \Delta h_i] + \Sigma_i (D_i/2)(\Delta h_i)^2$, i.e., compared to the functional integral Eq. (7) we have to introduce an additional harmonic potential term for the deviation Δh_i of the colloid position from its equilibrium value $h_{i,\mathrm{eq}}$ in the expression for the partition function describing the thermal fluctuations of the interface and the colloids. The additional potential term $V_i = (D_i/2)(\Delta h_i)^2$, which is centered at $\Delta h_i = 0$, can be included in the boundary Hamiltonians $\mathcal{H}_{i,\mathrm{b}}$ and leads to additional terms in the self-energy parts of Eq. (33) for the mean-field part of the partition function. The integrals over the Δh_i and the boundary multipoles can be performed as before. The additional potentials V_i lead to modifications of the determinant of the matrix $\mathbf{E}$. Because of the different form of integration measure for the cases of a pinned and an unpinned contact line (cf. Sec. II A), these modifications differ for the two types of boundary conditions. For the leading term of the mean-field Casimir force we can write

$$F_{\mathrm{mf}} \overset{\lambda_c \to \infty}{=} \frac{k_B T}{2}\frac{1}{d \ln d/r_0}\frac{1}{1 + \dfrac{o_1 o_2 \ln(d/r_0)}{o_1 + o_2}}, \tag{63}$$

where $o_i = D_i/(\pi\gamma)$ for a pinned contact line and $o_i = 2/(1 + 2\pi\gamma/D_i)$ for an unpinned contact line. So the inclusion of the harmonic potential leads to a decreased mean-field contribution to the fluctuation-induced force as compared to Eq. (37) which decreases with increasing strength D_i of the potentials (see Fig. 5). For a pinned contact line, in this way the leading term of mean-field contribution to the Casimir force can be switched on in a controlled way by an external harmonic potential. In the limit $D_i \to 0$ we recover for both cases the result from Sec. III B, Eq. (37), which gives rise to the cancellation of the leading terms with those of the fluctuation part. This is expected because $D_i = 0$ corresponds to the cases (A), (B2), or (B3) where height fluctuations of the colloids are not suppressed by external potentials. In the opposite limit $D_i \to \infty$, however, we find $F_{\mathrm{mf}} \to 0$ from Eq. (63) for a pinned contact line. This corresponds to case (B1) of frozen colloid positions and a pinned contact line and where the full Casimir force is given by the fluctuation part Eq. (23). In the case of an unpinned contact line, this effect is less pronounced. Then the original form of the mean-field Casimir force, Eq. (37), is diminished by an additional factor $1/(1 + \ln d/r_0)$ in the limit $D_i \to \infty$.

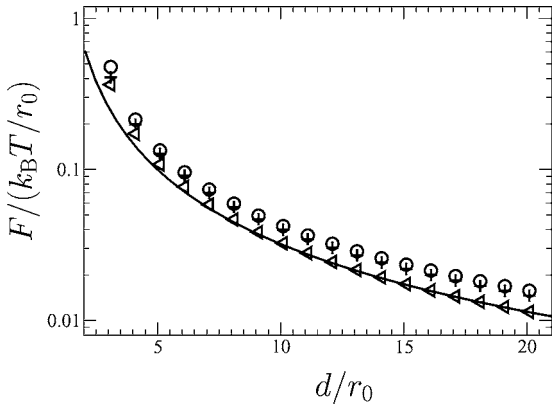

FIG. 5. Numerical calculation of mean-field part F_{mf} of the Casimir force with harmonic external potential for the colloids for $D_i/\gamma=1$ [triangles, compared to the analytical result Eq. (63) solid line] and $D_i/\gamma=0.1$ (pluses) in the case of pinned contact line. The circles show the fluctuation part $-F_{fluc}$ of the Casimir force, which has to be added to F_{mf} to obtain the total force. As can be seen from the plot, for increasing D_i/γ the fluctuation part becomes dominant.

For the linear external potential (constant force on the colloids)—also relevant for a harmonic potential with relatively large displacement—the only effect is an additional capillary interaction to the fluctuation-induced force. The relative importance of these two contributions to the colloid interaction is determined by their amplitudes F_i^2/γ and k_BT, respectively. For a harmonic external potential, the relevance of the external potential on both the classical capillary interaction [cf. Eqs. (60)–(62)] and on the fluctuation-induced force Eq. (63) is governed by the ratio γ/D_i of the surface tension and the stiffness D_i of the harmonic potential. For typical values for the surface tension in the range of $\gamma \simeq 10$ mN/m and a stiffness $D_i \simeq 10^{-3}-1$ mN/m [35] of the harmonic potential, we find that the classical interaction can be neglected compared to the fluctuation force (whose strength is governed by k_BT), but, also, the effect of the external potential on the Casimir force is marginal. For steeper harmonic potentials or lower surface tensions (cf., e.g., Ref. [36]), such that $\gamma/D_i \leqslant 1$, we find an increasing influence of the the external potential. Then the mean-field part F_{mf} of the fluctuation induced force is considerably decreased which leads to a more attractive total Casimir force because the fluctuation part then will dominate F_{mf} (cf. Sec. III). On the other hand, in this regime also the classical capillary interaction reaches the magnitude of the fluctuation induced force.

VII. SUMMARY

The restrictions that two rotational symmetric colloids trapped at a fluid interface impose on the thermally excited interfacial fluctuations (capillary waves) by their sheer presence lead to a thermal Casimir force. This effective fluctuation force can be calculated both numerically in the whole range of colloid separations d and analytically for the asymptotic ranges of either small or large separations. In the present effort we have done this using two approaches. Thereby we find the following results.

(1) The decomposition of the interfacial partition function into a part describing colloid fluctuations on a mean-field interface and a part describing the interface fluctuations facilitates the calculation of the fluctuation force both numerically in the whole range of colloid separations d and analytically for small (large) d. In the long-range limit $d \gg r_0$, one observes an interesting interplay between the attractive interaction from the interface fluctuations and a repulsive interaction caused by the fluctuating colloid. This results in a cancellation of the leading terms up to a certain order in $1/d$, which is determined by the specific model considered for the boundary conditions. In the case of like boundary conditions on the two colloids, we find that in the case of freely fluctuating colloids—with either a pinned (B3) or unpinned (A) contact line—the Casimir force is characterized by a fast decay $\propto -d^{-9}$. For a pinned contact line, fixing colloidal degrees of freedom leads to longer-ranged forces which are $\propto -d^{-5}$ (if only the orientation of the colloids is fixed) and $\propto -1/d \ln d$ (if both orientation and vertical position are fixed). In the case of mixed boundary conditions we find a repulsive total Casimir in the long-range limit if a pinned and a unpinned contact line are combined.

(2) This cancellation of the leading terms for these two parts can be understood in an alternative approach (that is unsuitable for a numerical solution, however) in which the analogy of the effective Hamiltonian to electrostatics is exploited. In this approach the fluctuation-induced force can be interpreted in terms of an interaction between fluctuating auxiliary multipole moments defined on the area enclosed by the contact line of the colloids. The various boundary conditions at the three phase contact line translate into conditions for the auxiliary multipoles. The asymptotics of the fluctuation induced force for intermediate colloid separations then is determined by the interaction of the leading nonvanishing auxiliary multipoles.

(3) In the opposite limit of a close colloid-colloid separation $h=d-2r_0 \ll r_0$, the effect of the boundary conditions is much less pronounced. Both the mean-field and the fluctuation parts diverge for $h \to 0$, but the resulting force is dominated by $F_{fluc} \sim h^{-3/2}$ (compared to $F_{mf} \sim h^{-1}$), leading to a strong Casimir interaction in this regime for all combinations of boundary conditions (cf. Fig. 4).

(4) For typical values in experimental situations, the fluctuation force will dominate classical capillary forces arising from meniscus deformations by an external potential. Nevertheless, such external potentials provide the possibility to tune the fluctuation force directly or to superimpose classical and fluctuation forces by a sophisticated choice of the experimental setting.

All our analysis has been concerned with static effects. New effects may be expected if colloid-colloid correlations on the interface can be measured and calculated dynamically since the time scale associated with the colloid fluctuations (Brownian motion) is quite independent from that of interface fluctuations (overdamped capillary waves). Here we would expect strong signatures from both types of fluctuations (albeit on different time scales) unlike in the present analysis where the effects of interface and colloid fluctuations (for a free colloid) cancel each other at long distances.

Experimental efforts in this direction are currently under way [37] and hopefully will stimulate further theoretical work.

APPENDIX A: THE BOUNDARY HAMILTONIAN $\mathcal{H}_{i,b}$

From Eq. (4) we find that the boundary Hamiltonians $\mathcal{H}_{i,b}$ consists of three parts. In this appendix we show how $\mathcal{H}_{i,b}$ can be expressed in terms of the boundary multipole moments P_{im}, leading to the second-order expansion given in Eq. (4). For the case (A) of spherical colloids and a fluctuating contact line all areas $\Delta A_{I(II)}$ and ΔA_{proj} are nonzero. For the case (B3) of a pinned contact line (disks or Janus spheres), $\Delta A_{I(II)}=0$ and the boundary Hamiltonians are fully determined by the change in the projected meniscus area ΔA_{proj}. [For the remaining cases (B1) and (B2) all area changes vanish and thus the boundary Hamiltonian is zero.] It is sufficient to determine the area changes $\Delta A'_{I(II)}=0$ and $\Delta A'_{proj}$ for a single colloid; the total area changes are just given by a sum of these.

If the three phase contact is slowly varying without overhangs it can be written as a function of polar angle φ, and for sperical colloids its distance to the z axis is given by

$$r_0(\varphi) = \sqrt{R^2 - [h_0 + u(r_0(\varphi))]^2} = \sqrt{r_0^2 - 2R\cos\theta u(r_0(\varphi)) - u(r_0(\varphi))^2}, \quad \text{(A1)}$$

where $u(r_0(\varphi))$ is the height of the three-phase contact line, and $h_0=-R\cos\theta$ is the height of the colloid center in the reference configuration (cf. Sec. II). For the second equality we have have used $r_0=R\sin\theta$.

Following Appendix A in Ref. [13], we parametrize the projection of the actual three-phase contact line onto the reference plane in terms of the polar angle φ and write (h is the change in vertical position of the colloid center with respect to the reference configuration)

$$\gamma_I\Delta A'_I + \gamma_{II}\Delta A'_{II} = \frac{\gamma}{2}\int_0^{2\pi} d\varphi[u(r_0(\varphi)) - h]^2 + \frac{\gamma}{2}\int_0^{2\pi} d\varphi[r_0^2(\varphi) - r_0^2] \simeq \frac{\gamma}{2}\int_0^{2\pi} d\varphi[f-h]^2 + \frac{\gamma}{2}\int_0^{2\pi} d\varphi[r_0^2(\varphi) - r_0^2], \quad \text{(A2)}$$

where in the first term in the second relation we have replaced $u(r_0(\varphi))\simeq u(r_0,\phi)\equiv f$, i.e., we have replaced the contact line height by the meniscus height at the reference contact circle, since this approximation produces only terms which are at most of third order in the boundary multipoles. The second contribution to $\mathcal{H}_b$ stems from the changes in the projected meniscus area and can be written as

$$\gamma\Delta A'_{proj} = \gamma\int_0^{2\pi} d\varphi\int_{r_0(\varphi)}^{r_0} drr = \frac{\gamma}{2}\int_0^{2\pi} d\varphi[r_0^2 - r_0^2(\varphi)]. \quad \text{(A3)}$$

In case (A), $\Delta A'_{I(II)}\neq 0$, and both Eqs. (A2) and (A3) are contributing to $\mathcal{H}_{i,b}$, leading to a cancellation of the contribution from the change in the projected meniscus area of Eq. (A3) by the second term in Eq. (A3). Inserting the decomposition of $f(\varphi)$ from Eq. (3) (omitting the colloid label i) we find

$$H_b \simeq \frac{\gamma}{2}\int_0^{2\pi} d\varphi[f(\varphi)-h]^2 = \frac{\pi\gamma}{2}\left(2(P_0-h)^2 + 4\sum_{m\geq 1}|P_m|^2\right). \quad \text{(A4)}$$

For the case (B3) there are also tilt fluctuations of the vertical axis of the three-phase contact line circle which can be parametrized by a boundary height according to $f=P_1e^{i\varphi}+P_{-1}e^{-i\varphi}$, the projection of the tilted circle onto the reference plane $z=0$ is an ellipse, and we find for the boundary Hamiltonian according to Eq. (A3)

$$H_b \simeq \pi\gamma(|P_1|^2 + |P_{-1}|^2). \quad \text{(A5)}$$

Note, however, that we can write $\mathcal{H}_{b,i}$ as in Eq. (4) for all cases for the boundary conditions, (A) and (B1)–(B3), since the integration measure $\mathcal{D}f_i$ for the contact line is constructed such that only the actual terms for the respective cases contribute (see Sec. II A).

APPENDIX B: EXPANSION OF THE GREEN'S FUNCTION

In this appendix we derive the multipole expansion of the Green's function $G(|\mathbf{x}|)\approx -(1/2\pi)\ln(\gamma_e|\mathbf{x}|/2\lambda_c)$ between two "charged" (charges generating the auxiliary field ψ_i) and isolated regions ($\partial S_{i,ref}$ in Sec. III A and $S_{i,ref}$ in Sec. III C). The method we apply is known from electrostatics and goes back to Schwinger (cf. [38]) and is referred to as the Schwinger technique in the literature. In doing so, we use the analogy of our problem to two-dimensional electrostatics. As starting point we use the fact that the logarithm is the generating function of the Gegenbauer polynomials. Using $|\mathbf{r}-\mathbf{r}'| = \sqrt{r^2+r'^2-2rr'\cos(\varphi-\varphi')}$ and exploiting some properties of the Gegenbauer polynomials [39], we find

$$\ln|\mathbf{r}-\mathbf{r}'| = \ln r + \sum_{l\geq 1}\frac{1}{l}\left(\frac{r'}{r}\right)^l\cos(l\varphi - l\varphi'), \quad \text{(B1)}$$

where we assumed $r'=|\mathbf{r}'|<r=|\mathbf{r}|$. Comparing Eq. (B1) to the Taylor expansion of the logarithm, we find

$$\frac{(-\mathbf{r}'\cdot\boldsymbol{\nabla})^l}{l!}\ln r = \begin{cases}\ln r, & l=0,\\ -\dfrac{1}{2l}\left(\dfrac{r'}{r}\right)^l(e^{i(l\varphi-l\varphi')}+e^{-i(l\varphi-l\varphi')}), & l>0.\end{cases} \quad \text{(B2)}$$

On the other hand, introducing $\xi_\pm=\partial_x\pm i\partial_y$ and using $\xi_+\xi_-\ln r=\xi_-\xi_+\ln r=0$, we can write

$$\frac{(-\mathbf{r}'\cdot\boldsymbol{\nabla})^l}{l!}\ln r=\frac{(-1)^l}{l!}\left(\frac{r'}{2}\right)^l(e^{-il\varphi'}\xi_+^l+e^{il\varphi'}\xi_-^l)\ln r. \tag{B3}$$

Identifying Eqs. (B1) and (B3) we obtain

$$\xi_\pm^l\ln r=-(-2)^{l-1}(l-1)!\frac{e^{\pm il\varphi}}{r^l}. \tag{B4}$$

With Eq. (B4) at hand and for $\mathbf{x}_1=\mathbf{r}_1$ and $\mathbf{x}_2=\mathbf{d}+\mathbf{r}_2$ residing on different circles we obtain for the Green's function $G(|\mathbf{x}_2-\mathbf{x}_1|)$

$$\begin{aligned}
&-\frac{1}{2\pi}\ln\left(\frac{\gamma_e|\mathbf{d}+\mathbf{r}_2-\mathbf{r}_1|}{2\lambda_c}\right)\\
&\quad=-\frac{1}{2\pi}\ln\left(\frac{\gamma_e d}{2\lambda_c}\right)+\frac{1}{2\pi}\sum_{\substack{l_1,l_2=0\\ l_1+l_2\geqslant 1}}\frac{(-\mathbf{r}_1\cdot\boldsymbol{\nabla})^{l_1}}{l_1!}\frac{(\mathbf{r}_2\cdot\boldsymbol{\nabla})^{l_2}}{l_2!}\ln r\\
&\quad=-\frac{1}{2\pi}\ln\left(\frac{\gamma_e d}{2\lambda_c}\right)+\frac{1}{2\pi}\sum_{\substack{l_1,l_2=0\\ l_1+l_2\geqslant 1}}\frac{(-r_1)^{l_1}r_2^{l_2}}{l_1!l_2!2^{l_1+l_2}}\\
&\qquad\times(e^{-i(l_1\varphi_1+l_2\varphi_2)}\xi_+^{l_1+l_2}+e^{i(l_1\varphi_1+l_2\varphi_2)}\xi_-^{l_1+l_2})\ln r\\
&\quad=-\frac{1}{2\pi}\ln\left(\frac{\gamma_e d}{2\lambda_c}\right)+\frac{1}{2\pi}\sum_{\substack{l_1,l_2=0\\ l_1+l_2\geqslant 1}}\frac{(-1)^{l_1}}{l_1+l_2}\binom{l_1+l_2}{l_1}\frac{r_1^{l_1}r_2^{l_2}}{2d^{l_1+l_2}}\\
&\qquad\times(e^{-i(l_1\varphi_1+l_2\varphi_2)}+e^{i(l_1\varphi_1+l_2\varphi_2)}).
\end{aligned} \tag{B5}$$

In Sec. III A we also need the multipole expansion of $G(|\mathbf{x}_2-\mathbf{x}_1|)$ for $\mathbf{x}_i$ residing on the circumference $\partial S_{i,\mathrm{ref}}$ of the same circle in order to calculate the elements of the self-energy matrix, Eq. (18). Using Eq. (B1), we obtain with $|\mathbf{x}_1-\mathbf{x}_2|=r_0\sqrt{2-2\cos(\varphi_1-\varphi_2)}$

$$\begin{aligned}
G(|\mathbf{x}_1-\mathbf{x}_2|)&\simeq-\frac{1}{2\pi}\ln\left(\frac{\gamma_e r_0}{2\lambda_c}\right)-\frac{1}{2\pi}\ln[1-\cos(\varphi_2-\varphi_1)]\\
&=-\frac{1}{2\pi}\ln\left(\frac{\gamma_e r_0}{2\lambda_c}\right)+\frac{1}{2\pi}\sum_{l\geqslant 1}\frac{1}{2l}(e^{il\varphi_1-il\varphi_2}\\
&\quad+e^{-il\varphi_1+il\varphi_2}).
\end{aligned} \tag{B6}$$

Here the prerequisite $r'<r$ of Eq. (B1) is not satisfied, and the series in Eq. (B6) is not convergent. It has to be understood in a formal sense, since it only provides the Fourier coefficients for a finite number of modes which actually contribute to the effective interaction in the long-range regime (see Sec. III A for details).

APPENDIX C: KARDAR'S METHOD: CALCULATION OF THE SELF-ENERGY

The self-energy part, Eq. (46), is evaluated quite similarly as in Ref. [20]. We eliminate the δ functions by introducing conjugate multipole moments $\tilde{\Psi}_{im}$ of the auxiliary fields:

$$\begin{aligned}
&\delta\left(\Psi_{im}-\int_{S_{i,\mathrm{ref}}}d^2x(r/r_0)^{|m|}e^{-im\varphi}\psi(\mathbf{x})\right)\\
&\quad=\int d\tilde{\Psi}_{im}\exp\left[i\tilde{\Psi}_{im}\left(\Psi_{im}\right.\right.\\
&\qquad\left.\left.-\int_{S_{i,\mathrm{ref}}}d^2x(r/r_0)^{|m|}e^{-im\varphi}\psi_i(\mathbf{x})\right)\right].
\end{aligned} \tag{C1}$$

This brings $Z_{\mathrm{i,self}}=\exp\{-k_BT/(2\gamma)\mathcal{H}_{i,\mathrm{self}}\}$ into the form

$$\begin{aligned}
Z_{\mathrm{i,self}}=\int\prod_m d\tilde{\Psi}_{im}\int D\psi_i\exp\Bigg(&-\frac{k_BT}{2\gamma}\int_{S_{i,\mathrm{ref}}}\\
&\times d^2x\int_{S_{i,\mathrm{ref}}}d^2x'\,\psi_i(\mathbf{x})G(|\mathbf{x}-\mathbf{x}'|)\psi_i(\mathbf{x})\\
&-i\int_{S_{i,\mathrm{ref}}}d^2x\psi_i(\mathbf{x})\sum_m\left(\frac{r_i}{r_0}\right)^{|m|}(P_{im}+\tilde{\Psi}_{im})e^{im\varphi_i}\\
&+i\sum_{m=-\infty}^{\infty}(P_{im}+\tilde{\Psi}_{im})\Psi_{im}\Bigg).
\end{aligned} \tag{C2}$$

The functional integral $\int\mathcal{D}\psi_i$ in Eq. (C2) can be converted into a functional integral over a constrained height field $h(\mathbf{x})$; this corresponds to a reversion of the step from Eq. (14) to Eq. (42),

$$\begin{aligned}
Z_{i,\mathrm{self}}=\int\prod_m d\tilde{\Psi}_{im}\exp\left(i\sum_{m=-\infty}^{\infty}(P_{im}+\tilde{\Psi}_{im})\Psi_{im}\right)\int\mathcal{D}h\\
\times\prod_{\mathbf{x}_i\in S_{i,\mathrm{ref}}}\delta\left(h(\mathbf{x}_i)-\sum_m\left(\frac{r_i}{r_0}\right)^{|m|}(P_{im}+\tilde{\Psi}_{im})e^{im\varphi_i}\right)\\
\times\exp\left[-\frac{\gamma}{2k_BT}\int d^2x\left((\boldsymbol{\nabla}h)^2+\frac{h^2}{\lambda_c^2}\right)\right].
\end{aligned} \tag{C3}$$

In Eq. (C3), the δ functions describe the pinning of the field h in the region $S_{i,\mathrm{ref}}$. This contribution can be evaluated directly, such that the remaining functional integral reads

$$\begin{aligned}
Z_{\mathrm{i,self}}\overset{\lambda_c\to\infty}{\approx}&\int\prod_m d\tilde{\Psi}_{im}\exp\left(-\frac{2\pi\gamma}{k_BT}\sum_{m\geqslant 1}m|P_{im}+\tilde{\Psi}_{im}|^2\right.\\
&\left.+i\sum_m(P_{im}+\tilde{\Psi}_{im})\Psi_{im}\right)\int\mathcal{D}h\prod_{\mathbf{x}_i\in\partial S_{i,\mathrm{ref}}}\delta(h(\mathbf{x}_i)\\
&-\sum_m(P_{im}+\tilde{\Psi}_{im})e^{im\varphi_i})\\
&\times\exp\left[-\frac{\gamma}{2k_BT}\int_{\mathbb{R}^2\setminus S_{i,\mathrm{ref}}}d^2x\left((\boldsymbol{\nabla}h)^2+\frac{h^2}{\lambda_2^2}\right)\right],
\end{aligned} \tag{C4}$$

where the δ functions fix $h(\mathbf{x})$ at the boundaries $\partial S_{i,\mathrm{ref}}$ of the integration domain. Splitting the auxiliary field into two parts as in Eq. (8), $h=h_0+h_1$, where $(-\Delta+\lambda_c^{-2})h_0=0$ with the boundary conditions $h_0(\mathbf{x}_i)|_{\partial S_{i,\mathrm{ref}}}=\Sigma_{m=-\infty}^{\infty}(P_{im}+\tilde{\Psi}_{im})e^{im\varphi_i}$ and $h_1(\mathbf{x}_i)|_{\partial S_{i,\mathrm{ref}}}=0$, and applying Gauss's theorem to the integral in the exponent of Eq. (C4) leads to

$$Z_{\mathrm{i,self}} = \int \prod_m d\tilde{\Psi}_{im} \exp\left(- \frac{2\pi\gamma}{k_B T} \sum_{m\geqslant 1} |m| |P_{im} + \tilde{\Psi}_{im}|^2 + i \sum_{m=-\infty}^{\infty} (P_{im} + \tilde{\Psi}_{im}) \Psi_{im} \right) \times \exp\left(- \frac{\gamma}{2k_B T} \oint_{\partial S_{i,\mathrm{ref}}} d\mathbf{x}\, h_0(\mathbf{x})\, \boldsymbol{\nabla} h_0(\mathbf{x}) \right) \times \int Dh_1 \prod_{\mathbf{x}\in\partial S_{i,\mathrm{ref}}} \delta(h_1(\mathbf{x})) \times \exp\left[- \frac{k_B T}{2\gamma} \int_{\mathbb{R}^2\setminus S_{i,\mathrm{ref}}} d^2x \left((\boldsymbol{\nabla} h_1)^2 + \frac{h_1^2}{\lambda_c^2} \right) \right]. \quad \text{(C5)}$$

The functional integral over h_1 only yields a constant factor independent of any multipole moment, which will be disregarded below. To compute the line integral in Eq. (C5), we write the general solution of the differential equation for h_0 in $\mathbb{R}^2\setminus S_{i,\mathrm{ref}}$ as (cf. Sec. III B) $h_0(\mathbf{x}) = \Sigma_m [K_m(r/\lambda_c)/K_m(r_0/\lambda_c)] C_m e^{im\varphi}$. By comparison to the boundary conditions the coefficients are determined straightforwardly as $C_m = P_{im} + \tilde{\Psi}_{im}$. Then, the line integral evaluates to $2\pi |P_{im} + \tilde{\Psi}_{im}|^2 f(m)$ with $f(m) = |m| (|m| \geqslant 1)$ and $f(0) = -1/\ln(\gamma_e r_0/2\lambda_c)$, such that the self-energy part reads

$$Z_{i,\mathrm{self}} = \int \prod_m d\tilde{\Psi}_{im} \exp\left(- \frac{4\pi\gamma}{k_B T} \sum_{m\geqslant 0} \frac{f(m)}{1+\delta_{m0}} |P_{im} + \tilde{\Psi}_{im}|^2 + i \sum_{m=-\infty}^{\infty} (P_{im} + \tilde{\Psi}_{im}) \Psi_{im} \right) \quad \text{(C6)}$$

and thus $\mathcal{H}_{i,\mathrm{self}}$ is given by (up to unimportant additive constants)

$$H_{i,\mathrm{self}} = \sum_{m\geqslant 1} |\Psi_{im}|^2 \frac{1}{2\pi f(m)}. \quad \text{(C7)}$$

[1] J. D. Joannopoulos, Nature (London) **414**, 257 (2001).
[2] P. Pieranski, Phys. Rev. Lett. **45**, 569 (1980).
[3] F. Ghezzi and J. C. Earnshaw, J. Phys.: Condens. Matter **9**, L517 (1997).
[4] F. Ghezzi, J. C. Earnshaw, M. Finnis, and M. McCluney, J. Colloid Interface Sci. **238**, 433 (2001).
[5] J. Ruiz-Garcia and B. I. Ivlev, Mol. Phys. **95**, 371 (1998).
[6] J. Ruiz-Garcia, R. Gamez-Corrales, and B. I. Ivlev, Phys. Rev. E **58**, 660 (1998).
[7] D. Stamou, C. Duschl, and D. Johannsmann, Phys. Rev. E **62**, 5263 (2000).
[8] M. Quesada-Perez, A. Moncho-Jorda, F. Martinez-Lopez, and R. Hidalgo-Alvarez, J. Chem. Phys. **115**, 10897 (2001).
[9] R. P. Sear, S.-W. Chung, G. Markovich, W. M. Gelbart, and J. R. Heath, Phys. Rev. E **59**, R6255 (1999).
[10] W. Chen, S. Tan, T.-K. Ng, W. T. Ford, and P. Tong, Phys. Rev. Lett. **95**, 218301 (2005).
[11] M. G. Nikolaides, A. R. Bausch, M. F. Hsu, A. D. Dinsmore, M. P. Brenner, C. Gay, and D. A. Weitz, Nature (London) **424**, 1014 (2003).
[12] A. Würger and L. Foret, J. Phys. Chem. B **109**, 16435 (2005).
[13] M. Oettel, A. Dominguez, and S. Dietrich, Phys. Rev. E **71**, 051401 (2005).
[14] M. Oettel, A. Domiguez, and S. Dietrich, J. Phys.: Condens. Matter **17**, L337 (2005).
[15] M. Oettel, J. Phys.: Condens. Matter **17**, 429 (2005).
[16] R. A. McGough and M. D. Miller, Phys. Rev. A **34**, 457 (1986).
[17] A. Kovalenko, and F. Hirata, Phys. Chem. Chem. Phys. **7**, 1785 (2005).
[18] D. Jasnow, in *Phase Transitions and Critical Phenomena*, ed. by C. Domb and J. L. Lebowitz (Academic, London, 1986), Vol. 10.
[19] M. Kardar and R. Golestanian, Rev. Mod. Phys. **71**, 1233 (1999).
[20] R. Golestanian, M. Goulian, and M. Kardar, Phys. Rev. E **54**, 6725 (1996).
[21] M. Goulian, R. Bruinsma, and P. Pincus, Europhys. Lett. **22**, 145 (1993); **23**, 155(E) (1993).
[22] H. Lehle, M. Oettel, and S. Dietrich, Europhys. Lett. **75**, 174 (2006).
[23] R. Golestanian, Phys. Rev. E **62**, 5242 (2000).
[24] S. Safran, *Statistical Thermodynamics of Surfaces, Interfaces, and Membranes* (Westview Press, Boulder, CO, 1994).
[25] H. Kleinert, *Path Integrals in Quantum Mechanics, Statistics and Polymer Physics*, 2nd ed (World Scientific, Singapore, 1995).
[26] M. Krech, *The Casimir Effect in Critical Systems* (World Scientific, Singapore, 1994).
[27] P. A. Kralchevsky, V. N. Paunov, I. B. Ivanov, and K. Nagayama, J. Colloid Interface Sci. **151**, 79 (1992).
[28] C. Bachas, P. Le Doussal, and K. J. Wiese, e-print hep-th/0606247.
[29] B. Derjaguin, Kolloid-Z. **69**, 155 (1934).
[30] H. Li and M. Kardar, Phys. Rev. Lett. **67**, 3275 (1991).
[31] H. Kaidi, T. Bickel, and K. Benhamou, Europhys. Lett. **69**, 15 (2005).
[32] R. Büscher and T. Emig, Phys. Rev. A **69**, 062101 (2004).
[33] W. H. Press, S. A. Teukolsky, W. T. Vetterling, and B. P. Flannery, *Numerical Recipes in C++*, 2nd ed (Cambridge University Press, Cambridge, U.K., 2002).
[34] C. Bauer, T. Bieker, and S. Dietrich, Phys. Rev. E **62**, 5324 (2000).
[35] L. Helden (private communication).
[36] D. G. A. l. Aarts, M. Schmidt, and H. N. W. Lekkerkerker, Science **304**, 847 (2004).
[37] C. Gutt (private communication).
[38] J. Schwinger, L. L. DeRaad, Jr., Kimball A. Milton, and Wuyang Tsai, *Classical Electrodynamics* (Perseus Books, Reading, MA, 1998).
[39] *Handbook of Mathematical Functions*, edited by M. Abramowitz and I. A. Stegun (Dover, New York, 1974).